# Geochemistry, Geophysics, Geosystems®

**RESEARCH ARTICLE**

**Key Points:**

- We present the 3D numerical model and observations related to the Africa-Arabia-Anatolian plume-rift system
- Our thermomechanical model provides new insight into the magma-rich intraplate active rifting in collisional settings
- Integrated analyses from the 3D geodynamic model and observations reveal a SW-NE-oriented plumelet and its regional implications

**Correspondence to:**

E. Şengül Uluocak,
ebrusengul@gmail.com

**Author Contributions:**

**Conceptualization:** Ebru Şengül Uluocak
**Formal analysis:** Ebru Şengül Uluocak, Andrea Sembroni
**Investigation:** Ebru Şengül Uluocak
**Methodology:** Ebru Şengül Uluocak
**Resources:** Russell N. Pysklywec
**Supervision:** Ebru Şengül Uluocak, Russell N. Pysklywec, Sascha Brune, Claudio Faccenna
**Visualization:** Ebru Şengül Uluocak
**Writing – original draft:** Ebru Şengül Uluocak
**Writing – review & editing:** Ebru Şengül Uluocak, Russell N. Pysklywec, Andrea Sembroni, Sascha Brune, Claudio Faccenna

# The Role of Upper Mantle Forces in Post-Subduction Tectonics: Plumelet and Active Rifting in the East Anatolian Plateau

**Ebru Şengül Uluocak[1,2]** , **Russell N. Pysklywec[3]** , **Andrea Sembroni[4]** , **Sascha Brune[2,5]** , and **Claudio Faccenna[2,4]**

[1]Department of Geophysical Engineering, Çanakkale Onsekiz Mart University, Çanakkale, Turkey, [2]Helmholtz Centre Potsdam—GFZ German Research Centre for Geosciences, Potsdam, Germany, [3]Department of Earth Sciences, University of Toronto, Toronto, ON, Canada, [4]Department of Science, Roma Tre University, Rome, Italy, [5]Institute of Geosciences, University of Potsdam, Potsdam, Germany

**Abstract** The spatiotemporal interaction of large- and regional-scale upper mantle forces can prevail in collisional settings. To better understand the role of these forces on post-subduction tectonics, we focus on mantle dynamics in the East Anatolian Plateau, a well-documented segment of the Arabian-Eurasian continental collision zone. Specifically, we analyze multiple forces in the upper mantle, which have not been considered in previous studies in this region. To this end, we use a state-of-the-art 3D instantaneous geodynamic model to quantify the dynamics of thermally defined upper mantle structures derived from seismic tomography data. Results reveal a prominent SW-NE-oriented mantle flow from the Arabian foreland to the Greater Caucasus–a plumelet–through a lithospheric channel under the East Anatolian Plateau. This plumelet induces localized dynamic topography (∼500 m) around the extensional Lake Van province, favoring NE-directed compression and westward escape of the Anatolian plate. We suggest that the Lake Van region is an active magma-rich intraplate rift in the Africa-Arabia-Anatolian plume-rift system. The rift zone was probably initiated by Neotethyan subduction-related forces and has been reactivated and/or sustained by the plumelet-induced convective support. Our findings are consistent with numerous observations, including the recent low-ultralow seismic velocities with a SW-NE splitting anisotropy pattern, geochemical and petrological studies, and local kinematics showing upper mantle-induced extensional tectonics in the collisional region.

**Plain Language Summary** Our goal is to better understand the active deformations of post-subduction tectonics. To this end, we ran a 3D thermomechanical model of the East Anatolian Plateau, one of the most intriguing segments of the Arabian-Eurasian continental collision zone. The model integrates seismically defined upper mantle structures and uses an open-source code (ASPECT). Results reveal the significant role of large- and regional-scale upper mantle forces in the study region. At long wavelengths, we find SW-NE-oriented mantle flow and associated dynamic topography. We interpret that such flow—a plumelet (regional upper-mantle plume migration with neither a significant tail extending to the lower mantle nor a mushroom head reaching the hot spots on the surface)—is linked to the large-scale mantle flow from the Arabian plate to the Greater Caucasus. At short wavelengths, we find localized dynamic topography and high stress and strain anomalies in the Lake Van zone. We argue that the plumelet, which became more forceful after the removal of the subducted Neotethyan slab, may have generated mantle tractions that contribute to magma-rich-intraplate rifting in the Lake Van region. Our results are in good agreement with local kinematics, low-speed seismic velocities with SW-NE anisotropy patterns, and geochemical-petrological studies.

## 1. Introduction

Plumes, fed by deep lower mantle sources mainly due to thermochemical instabilities, can have a considerable impact on mantle-lithosphere interactions, intraplate stresses, and crustal deformation (e.g., Burov & Gerya, 2014; Koptev et al., 2021; Steinberger & O'Connell, 1998). Seismic, numerical-analog modeling and plate reconstruction studies demonstrate that buoyant mantle bodies, with different shapes and spatial scales, can travel through the weak, thin lithosphere, accumulate below the lithosphere-asthenosphere boundary, and trigger the formation of continental rift zones (e.g., the East African and Red Sea rifts), high plateaus (e.g., Ethiopian and Kenyan Plateaus, Figure 1a), and large igneous provinces (e.g., Black et al., 2021; Burov & Guillou-Frottier, 2005; Civiero et al., 2022; Dannberg & Sobolev, 2015; Daradich et al., 2003; Ershov &
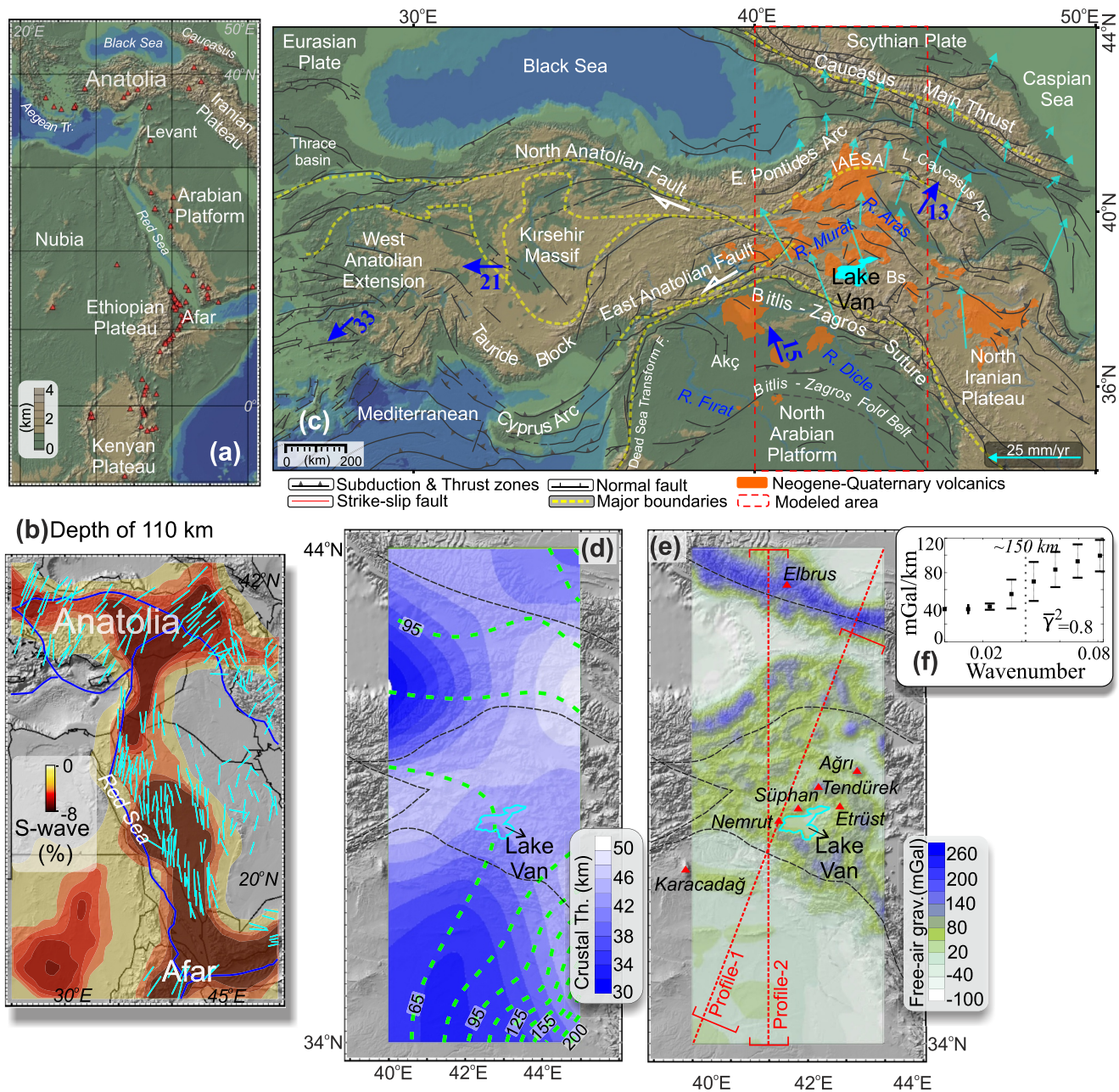
**Figure 1.** Major units and boundaries with isostatic topography analysis based on the admittance function of free-air and topography data in the study region. (a) Topography with major volcanic centers (red triangles) in the East African-Arabian-Anatolian region. (b) Shear-wave tomography slice for the depth of 110 km (Civiero et al., 2022) with splitting pattern (blue lines) based on seismic anisotropy models (Arvin et al., 2021; Civiero et al., 2022, 2023; Gao et al., 2010; Kaviani et al., 2021; Paul et al., 2014; Qaysi et al., 2018). (c) Simplified tectonic and geological units with major river systems in Turkey and surroundings. Blue arrows in (c) present the relative plate movement based on GPS studies (dark blue arrows show average values in cm/yr, Reilinger et al., 2006). (d) Crustal (color map) and lithospheric (contour map) variations in the study area (Priestley & McKenzie, 2013; Zor, 2008). (e) Free-air gravity data is shown as a color map (Bonvalot et al., 2012) over the topographic relief (black lines show the main fault and sutures). Triangles indicate Neogene-Quaternary volcanic centers. (f) Admittance and the average of the coherence values in the study area (Uluocak et al., 2021). Bs-Başkale and Akç-Akçakale graben zones, R-River, L-Lesser, IAESA-İzmir-Ankara-Erzincan-Sevan-Akera suture zone. Faults and boundaries are compiled from Kadinsky-Cade et al. (1981), Şengör and Yılmaz (1981), Okay et al. (2010), and Emre et al. (2018) (other references are given in the text). GMT 6 (Wessel et al., 2019), ParaView (Ahrens et al., 2005; Ayachit, 2015), Matlab (The MathWorks Inc, 2024, https://www.mathworks.com) and GeoMapApp (http://www.geomapapp.org, Ryan et al., 2009) were used to create figures in the study.

Nikishin, 2004; Faccenna et al., 2013; Hassan et al., 2020; Koppers et al., 2021; Maestrelli et al., 2022; Merle, 2011; Whitehead & Luther, 1975). Plumes can migrate horizontally away from their sources (up to several thousand kilometers), and their motion may be tracked by magmatic features that are formed due to

decompression melting of the upwelling hot mantle (e.g., Campbell & Griffiths, 1990; Civiero et al., 2022; Ershov & Nikishin, 2004; Hua et al., 2023; White & McKenzie, 1995). Geographically aligned volcanic centers with asthenospheric mantle-sourced geochemical components may therefore indicate the existence of a weak lithospheric corridor associated with underlying plumes. Long-wavelength upper mantle low/ultralow seismic velocity anomalies may manifest a weak lithospheric corridor (Figure 1b) for the propagation of the ascending mantle diapir (e.g., migration of a hot upper mantle plume, Ihinger, 1995). For example, such low-velocity zones have been observed from Kenya (Africa) to Elbrus (Caucasus), cutting across the Arabian-Eurasian collisional region (e.g., Becker & Boschi, 2002; Chang & Van der Lee, 2011; Civiero et al., 2022; Ershov & Nikishin, 2004; Faccenna et al., 2013). This region has been associated with a wide range of post-subduction deformation, shaping mobile belts and tectonics in the eastern Mediterranean realm since at least 20 Ma (Figure 1c, e.g., Faccenna et al., 2014; Pearce et al., 1990; Şengör & Yılmaz, 1981 and references therein).

The Cenozoic structure of eastern Anatolia—the active front of the Arabian-Eurasian collision—has been linked to the closure of the Neotethys Ocean that occurred between the Late Oligocene and Early Miocene (Şengör & Kidd, 1979; Şengör & Yılmaz, 1981). Lithospheric removal mechanisms, geochemical characteristics, and possible sources of magmatism have been the subject of numerous studies to explain the neotectonic evolution of this region (Memiş et al., 2020 and references therein). In particular, studies focused on (a) steepening and subsequent breaking-off of one (Faccenna et al., 2006; Keskin, 2003; Şengör et al., 2003) or two (Barazangi et al., 2006) northward-subducting Neotethys slab(s) under eastern Anatolia; (b) delamination of the lithospheric mantle (Göğüş & Pysklywec, 2008; Memiş et al., 2020) from the overlying thick East Anatolian crust; and (c) the large-scale implications of the East African plume (Ershov & Nikishin, 2004; Faccenna et al., 2013) accompanied by the subducted Aegean slab roll-back (Faccenna et al., 2013) in the collision zone. However, the proposed deformation scenarios do not fully explain the observed upper mantle heterogeneities and related post-subduction tectonics in the Eurasian-Arabian continental collisional region. In other words, the active forces underlying the large-scale low-velocity curtain anomaly in the region (Figure 1b, Civiero et al., 2019, 2023 and references therein), during the convergence between the Arabian-African and Eurasian plates, are still debated. To address these issues, we explore the migration of upper mantle features at long wavelengths as "plumelet"—that is, upper-mantle plume migration with neither a significant tail extending to the lower mantle nor a mushroom head reaching the hot spots on the surface. We quantify both the large- and regional-scale impact of mantle dynamics by conducting a geodynamic model based on the 3D instantaneous thermomechanical model configuration in the East Anatolian Plateau. Thermal states of the upper mantle structures from the North Arabian Platform to the Greater Caucasus have been previously interpreted by Uluocak et al. (2021) based on different seismic models. In this study, we focus on the Mediterranean-scale body-wave seismic tomography data (Piromallo & Morelli, 2003) to define stress, strain, temperature, and viscosity variations with dynamic topography and mantle flows that are mainly related to the seismically defined temperature field under the region. The numerical model provides an opportunity to understand the role of upper mantle heterogeneities in causing or controlling tectonic events at large and regional scales and the dynamical processes at work in collisional settings. Our results yield new insights into plumelet dynamics and associated surface expressions in collisional tectonics of the Mediterranean region and the Middle East.

## 2. Tectonic Setting: Constraints on Driving Forces

### 2.1. General Tectonic and Geological Features

The terminal collision of the Arabian plate with Eurasia along the Bitlis-Zagros thrust region in the southeast margin of Anatolia (Figure 1) occurred during the middle to early late Miocene and generated the high elevation and the recent tectonics of eastern Anatolia (Şengör et al., 2008 and references therein). This process formed two main suture zones, the Bitlis-Zagros and the İzmir–Ankara–Erzincan–Sevan-Akera suture zones, bounding the East Anatolian Plateau (Okay et al., 2010; Figure 1). In the region, active lithospheric subduction evolved into a continent-continent collision following the removal of the southern branch of the Neotethys oceanic slab beneath eastern Anatolia (e.g., Şengör & Kidd, 1979). This change in stress regime—from subduction to continental collision—is believed to have occurred at the end of the Early Pliocene (Şengör & Kidd, 1979), with precise timing estimated variably at: ~13-11 Ma (Faccenna et al., 2013; Keskin, 2003, 2007; Keskin et al., 1998; Şengör et al., 2008); before ~20 Ma (Schleiffarth et al., 2018); or between ~25–16.5 Ma (Rabayrol et al., 2019). In the Greater Caucasus, the active collision is accommodated by fold and thrust faults mainly parallel to the mountain ranges with different convergent rates that have been deduced by GPS measurements (blue arrow with average

values- ~13 mm/yr- in Figure 1c, Reilinger et al., 2006) and well-constrained kinematic studies (e.g., Van Hinsbergen et al., 2020 and references therein).

Geochemical and petrological studies indicate sustained volcanic activity over the last ~45 Ma in the volcanic belt stretching from Kenya in East Africa to the Elbrus in the Greater Caucasus (Figure 1a, Civiero et al., 2022, 2023; Ershov & Nikishin, 2004; Sharkov et al., 2015 and references therein). Late Cenozoic collision-related volcanism started in the plateau between ~8 and 6 Ma (Pearce et al., 1990 or at ~15 Ma; Lebedev et al., 2010; age compilation in Memiş et al. (2020)) following the initial rupture of the north-dipping Neotethyan slab during the active Arabian continental collision (e.g., Rabayrol et al., 2019). The intensified volcanic activity has been documented during the Pliocene—Quaternary times (Oyan et al., 2017) and has continued to historical periods in eastern Anatolia (e.g., Oyan et al., 2023). It has been interpreted that this rupture propagated westward with progressive sub-horizontal slab tearing (Bartol & Govers, 2014; Capitanio, 2016; Faccenna et al., 2006; Rabayrol et al., 2019).

The region is covered regionwide by thick Neogene-Quaternary volcanic-sedimentary rocks (Şengör & Yılmaz, 1981) with an Eocene–lower Miocene oceanic sedimentary unit, upper Cretaceous–Oligocene ophiolitic mélange and flysch, ~E-W trending folds and thrusts, and conjugate strike-slip faults (Keskin et al., 1998; Oyan et al., 2017; Pearce et al., 1990; Şengör et al., 2003, 2008; Topuz et al., 2017; Yılmaz et al., 1987; Figure 1c). Most of the volcanic rocks originated from the Nemrut, Süphan, Ağrı, Etrüks stratovolcanoes (early Pliocene-Quaternary in age) and Tendürek shield volcano (Quaternary in age, Aclan et al., 2020 and references therein), which are aligned on the plateau in a SW-NE direction (Figure 1e). The morphology of the Miocene Karacadağ in the Arabian foreland and the Quaternary Nemrut (last eruption at 1–0 Ma) in the plateau—the oldest and youngest volcanoes in the region—is characterized by N-S and E-W extensional fissures in the Akçakale and Başkale grabens, respectively (e.g., Lustrino et al., 2012; Pearce et al., 1990; Figures 1c and 1e). Analyses of Miocene to Quaternary basaltic lavas around the Lake Van region show an asthenospheric melting source enriched with different amounts of subduction components (Oyan et al., 2023 and references therein). This may indicate different tectonic stages of the plateau evolution associated with lithospheric detachment processes that resulted in a thin lithosphere beneath the relatively thick eastern Anatolian crust (Figure 1d).

## 2.2. Upper Mantle Forces of the Region

The regional geology in eastern Anatolia is consistent with an interpretation of post-subduction tectonics being controlled by either a weak, broken oceanic slab or an upwelling Arabian sub-slab asthenosphere (Rabayrol et al., 2019; Schleiffarth et al., 2018; Uslular & Gençalioğlu-Kuşcu, 2019). Petrological studies suggest that the entire thickened zone overlying an accretionary complex (Şengör & Kidd, 1979; Şengör et al., 2008) or continental basement (Topuz et al., 2017) may have been affected by lithospheric removal in the form of successive relatively small-scale or single-sudden detachments (Pearce et al., 1990). Different lithospheric removal scenarios have been proposed in the region (Keskin, 2007 and references therein). Regional numerical models by using a wide range of parameters (e.g., convergence rates, rheology, and origin of the materials) test delamination hypotheses quantitatively (Göğüş & Pysklywec, 2008; Memiş et al., 2020). These studies suggested that delamination of the mantle lithosphere (Göğüş & Pysklywec, 2008) or progressive removal of the northward-subducting Neotethys slab from eastern Pontides to the Bitlis-Zagros zone (i.e., gradual delamination/lithospheric peeling; Memiş et al., 2020) are viable mechanisms for driving surface uplift (up to 2 km) across the plateau (Figure 2a). Both delamination models consider the tectonics of the plateau without additional forces, for instance, a possible elastic rebound effect or convective support (i.e., flows from the south, Figure 2b) in response to the break-off of the Neotethyan slab (i.e., fall of subducted slab; Şengör et al., 2008). Thus, the evolution of magmatism and high topography is attributed simply to the delamination of the lithospheric layer and the upwelling of the mantle into the lithospheric gap beneath the east Anatolian crust (Göğüş & Pysklywec, 2008; Memiş et al., 2020).

Alternatively, elevated topography and asthenospheric temperatures inferred from geochemical data and drainage analyses across Anatolia (i.e., average uplift of ~0.4 mm/yr since 4 Ma and ~1673 K at 60 km depth, McNab et al., 2018) may be linked to lateral migration of a plume (Ershov & Nikishin, 2004; Faccenna et al., 2013; Kounoudis et al., 2020; Wilson et al., 2014), which can drive surface uplift and westward extrusion of Anatolia (Faccenna et al., 2013; Molin et al., 2023). Accordingly, a slab break-off may have activated mantle flows from the Arabian foreland in the south (Episode 2 in Figure 2a) that are suggested to turn westward under the plateau (i.e., from the Afar Plume, Faccenna et al., 2013). In contrast, studies on neotectonic deformation of the region
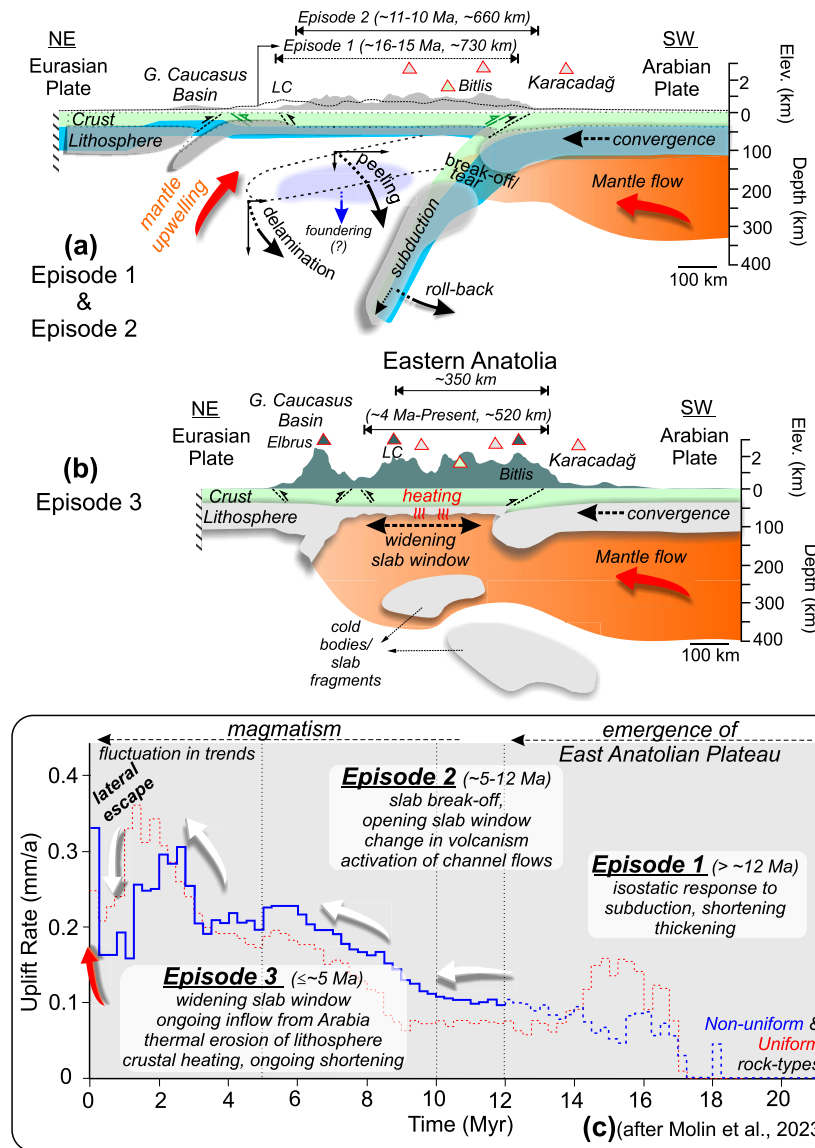
**Figure 2.** Model for the evolution of the formerly subducted slab and the uplift history of the East Anatolian Plateau. (a) Episodes 1 and 2 show isostatic response to the shortening and thickening of the Anatolian Plate, Neotethys slab break-off, opening of a window, and activation of the inflow from the Arabian foreland—termed plumelet in this study—(Molin et al., 2023). The blue arrow in the layer with a transparent background implies a conceptual model for the mechanical removal of the East Anatolian lithosphere mainly based on petrological and geochemical studies in the region (see a compilation of competing lithospheric foundering scenarios in Keskin, 2007 and references therein). (b) Episode 3 indicates the ongoing processes of Episode 2 with crustal heating. Notice that delamination scenarios suggest an upwelling mantle into the lithospheric gap that may generate the main uplift of the plateau without possible rebound effect or convective support in response to the slab break-off or tear (i.e., in response to detachment of the slab from the overlying plate by sub-horizontal rupture or sub-vertical rupture within the slab, respectively, e.g., Jolivet et al., 2015). The delamination hypothesis also supports the widening of the slab window with young volcanism projected onto SW-NE Profile-1 shown in Figure 1e. (c) Median uplift rates for non-uniform (blue) and uniform (red) rock types obtained from the Aras River longitudinal profile and inversion model (Molin et al., 2023). It should be stated that the confidence level of this model is higher at ages ≤12 Ma (see error bars in Molin et al. (2023)). Deformation processes presented here can overlap in time (see the text for further explanation and reference).

suggest that the westward drift of Anatolia might instead be governed by variations in gravitational potential energy from east to west across the plate (e.g., England & McKenzie, 1982) rather than by contribution from mantle convection or far-field effects of the Aegean slab rollback (e.g., England et al., 2016; McNab et al., 2018; Merry et al., 2021; Özeren & Holt, 2010). Recent analyses favor the boundary force argument for the initiation of

the westward escape of the plate along North and East Anatolian Transform Faults (Figure 1c), by neglecting any possible support by upper mantle convection (Şengör & Yazıcı, 2020). Those authors interpret that the main engine of the tectonic drift could be collisional forces caused by the impingement of the Arabian craton, resulting in the N-S crustal shortening and surface uplift in the East Anatolian Plateau during the last ~10 Ma (Şengör & Yazıcı, 2020 and references therein).

The contemporary elevation and its rate of change can help constrain active driving forces for tectonics in the region. Geomorphological studies on river network draining indicate a general non-equilibrium state and refer to the evolution of the plateau (Molin et al., 2023). Analyses of the fluvial terraces of the Murat River, an Euphrates-Fırat tributary flowing through the study region (Figure 1c), suggest ~800 m of surface uplift (~1,100 m of rock uplift) in the late Pliocene with an uplift rate of ~0.5 mm/a (Demir et al., 2009). Similar rates have been found in the Başkale Graben (southeast of the Lake Van province, Figure 1c) where morphometric analyses indicate a young topography and an active uplift with increasing rates from east to west in the graben system (Selçuk & Düzgün, 2017).

Analyses along the Aras River longitudinal profile and inversion models suggest three distinct phases of plateau uplift (Molin et al., 2023). In Episode 1 (Figure 2), the area was dominated by a low-relief landscape close to sea level uplifting with a rate of ~0.1 mm/a. The subsequent progressive emergence of the region could be associated with a renewed phase of exhumation in the middle-late Miocene with crustal shortening and thickening over the subducting slab (Episode 2, Figure 2a). A gradual increase in uplift rates (from ~0.1 to ~0.2 mm/a) is suggested between ~10 Ma and ~5 Ma (i.e., a trend in Episode 2 in Figures 2a and 2c), consistent with the proposed slab removal under the region. At ≤ ~5 Ma (Episode 3 in Figures 2b and 2c), when a ~30% decrease in convergence rates all over the region occurred (Cowgill et al., 2016), a dramatic increase in uplift rates (up to 0.3 mm/a) could be linked to the interaction between sub-crustal and crustal processes. This latter phase may involve processes such as the widening of the lithospheric window and the inflow of hot asthenospheric material from Arabia accompanying ongoing shortening and heating in the region (Elitok & Dolmaz, 2008; Molin et al., 2023). Molin et al. (2023) also interpret that the decreasing trend of the uplift rate at ~1 Ma can be related to the lateral movement of the Anatolian Plate (Figure 2c).

The recent rapid uplift (red arrow in Figure 2c) is consistent with 3D instantaneous geodynamic models that suggest an upper mantle-induced convective support on topography (~400 m–~1.2 km) in the East Anatolian Plateau (Uluocak et al., 2021). The present-day subcrustal mantle dynamics can also be interpreted from the ratio between free-air gravity (Figure 1e) and observed topography in the wavelength domain (i.e., admittance of ~40 mGal/km with high coherence - 0.8—at long wavelengths in Figure 1f, Uluocak et al., 2021), and from Airy-type crustal isostasy analyses, which all indicate non-isostatic components of the topography in the high plateau (Faccenna & Becker, 2010, 2020; Faccenna et al., 2014; Komut, 2015; Molin et al., 2023; Uluocak et al., 2021).

Seismic data give further insights into upper mantle structure and anomalously hot asthenosphere that may be related both to any lithospheric removal process and large-scale plate deformation (e.g., Fichtner et al., 2013; Kaban et al., 2018; Kounoudis et al., 2020; Lei & Zhao, 2007; Lü et al., 2017; Portner et al., 2018; Reid et al., 2019; Skobeltsyn et al., 2014; Zhu, 2018; Zor, 2008). P- and S-wave seismic tomography models in the East Anatolian Plateau, despite different waveforms, source frequencies, and resolutions, all show a low-velocity zone (the East Anatolian Slow EAS anomaly; Figure 3) at relatively shallow depths (≤~100 km, Kounoudis et al., 2020; Portner et al., 2018; Zor, 2008). The location of the EAS anomaly is supported by very low Pn-waves (≤7.8 km/s), indicating the presence of a shallow, hot asthenospheric mantle beneath the crust (Lü et al., 2017; Uluocak et al., 2021). The interaction between the low-velocity seismic zone and the crust is also in good agreement with high $Vp/Vs$ (≥1.9) values at the lower crust (Lin et al., 2020; Lü et al., 2017; Zhu, 2018), young volcanic areas (≤~6 Ma, around Nemrut and Süphan volcanoes, Figure 1e), and shallow Curie-point depths (e.g., 6–8 km in the north province of Lake Van; Oyan et al., 2017). Long-wavelength upper mantle low seismic velocity anomalies are observed in seismic tomography models extending from the Arabian plate to the Greater Caucasus (Figure 1b, Civiero et al., 2023; Piromallo & Morelli, 2003). Recent studies (Kounoudis et al., 2020; Portner et al., 2018) have imaged relatively small-scale high-velocity bodies (Figure 2b) under the plateau at depths up to ~200 km (Piromallo & Morelli, 2003). These are interpreted as slab fragments in the upper mantle (e.g., Dilek & Sandvol, 2006; Özacar et al., 2008; Portner et al., 2018).

In summary, there is a consensus on an absent or very thin lithospheric layer beneath the East Anatolian Plateau (Figure 1d) and, hence, the absence of a subducted oceanic slab that may decelerate or accelerate (e.g., rollback,
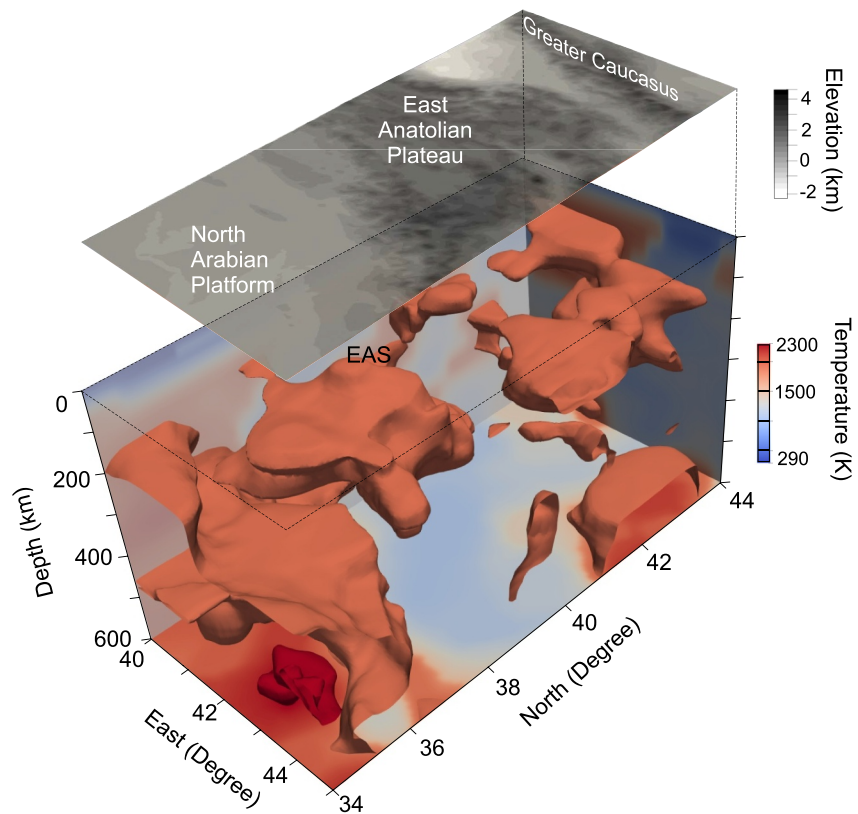
**Figure 3.** Input data for 3D thermomechanical geodynamic model. The model domain and mantle temperature structures used for the calculations (iso-contour shows temperature of 1950 K). The East Anatolian Slow anomaly (EAS) is located around the Lake Van region where the thinnest crust is observed under the plateau (the top panel shows topography variations, see text for further explanation and references).

pull) convergence or uplift rates in the region, at least since the end of Episode 2, as shown in Figure 2c. Different seismic-wave tomography models show a long-wavelength, low-velocity zone beneath the region between the Arabian foreland and the Greater Caucasus, which could be indicative of rising and migrating mantle flow—a plumelet—beneath the plateau. Observations and previous studies agree on upper mantle structures (Figure 2b) and crust-mantle interaction (e.g., the EAS anomaly; Figure 3) beneath the plateau. However, the role of upper mantle heterogeneities in causing or controlling tectonic events at large and regional scales in the continental collisional region, specifically in the East Anatolian Plateau (Figure 1), cannot be fully explained by previous numerical models. In this study, we use an instantaneous 3D thermomechanical model to analyze upper mantle forces to better understand the active deformations of post-subduction tectonics in the plateau.

## 3. Numerical Model

To investigate the mantle dynamics in the region, we conducted 3D instantaneous (present-day) geodynamic modeling (Figure 3, Table A1). The calculations were performed using the open-source ASPECT numerical code (version 2.4; Bangerth et al., 2019, 2022; Clevenger & Heister, 2021; Fraters et al., 2019; Glerum et al., 2018; Heister et al., 2017; Kronbichler et al., 2012; Rose et al., 2017). The code solves for the mechanical and thermal evolution of an incompressible medium, based on governing equations corresponding to the conservation of mass ($\nabla \cdot u = 0$), momentum ($\nabla \cdot \sigma_{ij} + \rho g = 0$), and energy $\rho C_p (\partial T/\partial t + u \cdot \nabla T) = k\nabla^2 T$, where $u$ is the velocity [m/s]; $g$ is the gravitational acceleration [9.8 m/s$^2$]; $k$ is thermal conductivity [W/m/K]; $T$ is the temperature [K]; $C_p$ is specific heat capacity [Jkg$^{-1}$K$^{-1}$]; $t$ is time [s]. The stress tensor ($\sigma_{ij} = \sigma'_{ij} - p\delta_{ij}$, [Pa]) can be defined by the deviatoric stress ($\sigma'_{ij}$) and the total pressure ($p$) (Pysklywec et al., 2000). In the numerical experiment, the plastic yield stress ($\sigma_y = p\sin\varphi$, where $\varphi$ is the internal angle of friction) and the viscous stress ($\sigma_v = 2\eta_e \dot{\varepsilon}$) determine the deviatoric stress; $\sigma'_{ij} = \min \{\sigma_y; \sigma_v\}$. The effective viscosity ($\eta_e$) in the viscous stress is defined for the power law creep based

on the temperature and the strain rate tensor $(\dot{\varepsilon})$; $\eta_e(\dot{\varepsilon}, T) = (1/2)\beta B^{-1/n}\dot{\varepsilon}^{(1-n)/n}\exp((Q + pV)/(nRT))$, where $n$ is the non-Newtonian viscosity exponent, $Q$ is the activation energy, $V$ is activation volume, $R$ is the universal gas constant ($8.31\,\mathrm{Jmol^{-1}K^{-1}}$), $B$ is the viscosity pre-factor, and $\beta$ is the scaling factor (Ranalli, 1995). We consider the Drucker-Prager yield criterion for rheological parameters in compositional fields shown in Table A1 (Appendix A). To investigate the deformation of the materials, the second invariant of the stress was obtained from the second invariant of the deviatoric stress tensor for the solution domain, as shown in Figure 3. Free slip for the sidewalls and bottom was set as the mechanical boundary conditions of the 3D model (e.g., Shaw & Pysklywec, 2007; Uluocak et al., 2016, 2019). A free surface was used at the top, which allows for the development of surface deflection (i.e., dynamic topography) caused by vertical stress imposed on the lithosphere by the underlying mantle (Uluocak et al., 2021 and references therein). Crustal heat production, relative plate motion, surface erosion and deposition were neglected in our calculations (Uluocak et al., 2021).

Temperature variations in the solution space were based on a Mediterranean-scale P-wave seismic tomography model (Piromallo & Morelli, 2003) calculated using the depth-dependent density scaling function of Karato (1993) with the thermal expansion rule; $\rho = \rho_0(1 - \alpha\Delta T)$, where $\rho_0$ is the reference density (see Table A1, Appendix A), $\alpha$ is the coefficient of thermal expansion $2 \times 10^{-5}$ [$\mathrm{K^{-1}}$], and $\Delta T$ is the temperature gradient. A reference geotherm that ranges from 293 to 1650 K for a depth of 600 km (Uluocak et al., 2021 and references therein) was used to calculate the absolute temperature field (Figure 3) together with the average values of the crustal and lithospheric thicknesses (i.e., ~40 and ~80 km, respectively, Figure 1d, Priestley & McKenzie, 2013; Zor, 2008). Experiments evolved with a small Courant–Friedrichs–Lewy (CFL, 0.1) number and a time up to ~$1 \times 10^5$ years, which are acceptable considering the relatively small-velocity errors (i.e., RMS ≤2 cm/year) for the effective computation time (Uluocak et al., 2021). For a more detailed discussion of the modeling methodology and parameters, the reader should refer to Uluocak (2023) and Bangerth et al. (2022).

## 4. Model Results and Tectonic Response to Mantle Dynamics

The present-day 3D thermomechanical model predicts a surface deflection with an average amplitude of ~+400 m at long wavelengths (≥150 km) caused by density/temperature–driven plumelet-style upper mantle flows (Figure 4a, Uluocak et al., 2021). The recent rapid uplift inferred from river network studies (~500 m, Figure 2c, Molin et al., 2023) and analyses of crustal isostasy at long-wavelengths (e.g., non-zero gravity admittance values in Figure 1e; Uluocak et al., 2021) are in good agreement with this first-order finding. The dynamic topography support is also compatible with different geodynamic model configurations (e.g., Faccenna et al., 2014; Komut, 2015; Uluocak et al., 2021). But different from these previous geodynamic modeling studies, we show modeling results that are sensitive to 3D regional upper mantle heterogeneities to interpret both large- and regional-scale dynamical processes in the region. Also, for the first time, we present regional 3D variations of stress, strain, velocity, and temperature fields in the study area with analyses of their regional implications.

The numerical results show negative buoyancy forces from relatively small-scale, shallow, cold anomalies beneath the region (blue iso-contour in Figure 4b). These structures are interpreted as detached Neotethys slab fragments and dense, cold, relatively thick lithospheric material observed under the northeastern part of the Arabian foreland (~−1.2 km) and the Black Sea (~−1 km) (Figure 4a). To the north of the study area, localized high dynamic topography values in Figure 4a are linked to upper mantle forces such as the upwelling mantle and active deformation in the Western Greater Caucasus-high and the Central Greater Caucasus-low (Uluocak et al., 2021).

We illustrate regional variations of temperature as a slice at 100 km depth and cross-section along Profile-1 with mantle flows for the range of 0–200 km depth in Figure 5. The yellow circle in Figure 5 shows localized mantle upwelling with increasing vertical amplitudes in vectors (i.e., black arrows) and high dynamic topography (up to ~500 m, Figures 4a and 6c) around the Lake Van region, including Nemrut and Süphan volcanoes in the north of the Bitlis-Zagros suture zone (Figure 1). This region correlates well with the location of the Van Anomaly (VA) shown in numerical results in Figure 4, the shallow/low-seismic/hot EAS anomaly (Figure 3), and young volcanoes (e.g., Nemrut, Figure 6) in the plateau. This anomaly is consistent with the general interpretation of lithospheric delamination models implying regional extension in the plateau (Göğüş & Pysklywec, 2008; Uluocak et al., 2021). Further, flows with smaller amplitudes shown in Figures 4 and 5 turn westward under eastern Anatolia. This result is compatible with the westward extrusion of Anatolia with respect to Eurasia and the
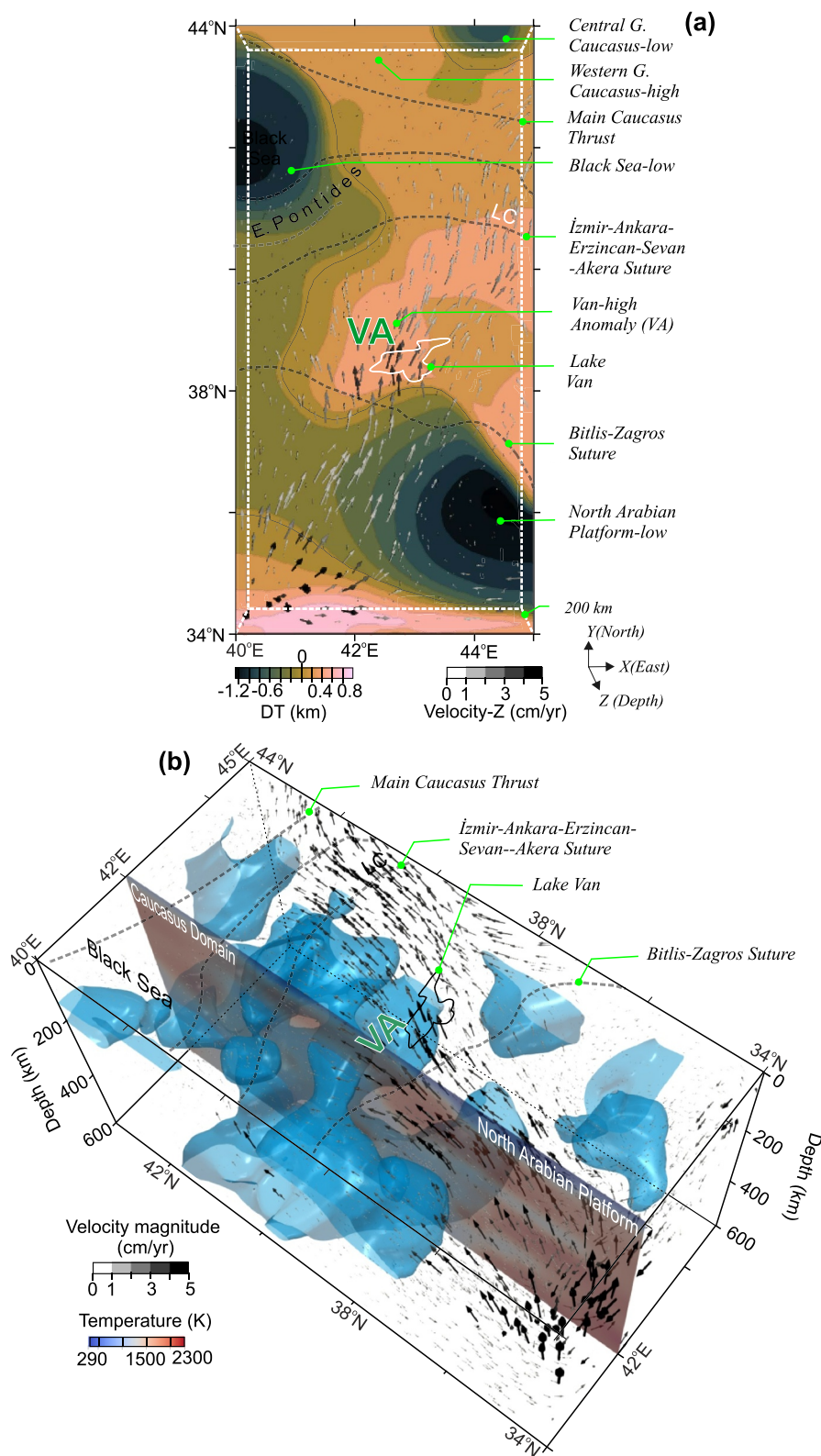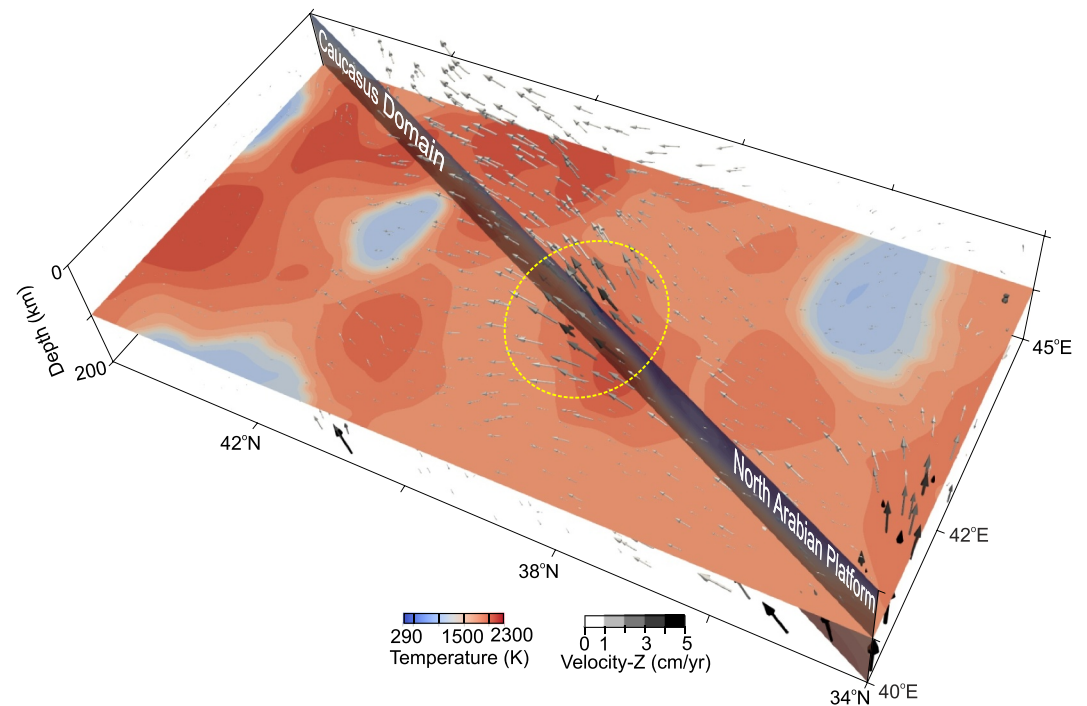
**Figure 4.**

**Figure 5.** Velocity vectors for the 0–200 km depth range and temperature variations. The temperature anomaly is shown as a slice at a depth of 100 km and along Profile-1. The dashed yellow circle shows the Lake Van extensional region where local upwellings into the lithospheric gap generate young volcanoes and rift tectonics (see Figure 4 for other abbreviations).

average variation of the surface wave seismic anisotropy model (<120 km) (Legendre et al., 2021; Reilinger et al., 2006; Uluocak et al., 2021).

We quantify stress and strain variations that may be associated with the observed active deformation in the region. Figure 6a shows a plan view of the second invariant of the stress field with the scaled maximum horizontal compressive stress ($SH_{max}$) for a depth of 40 km, the average value of the Moho surface depth in the model. Blue and green anomalies (i.e., vector fields) in Figure 6a indicate the difference between the maximal and minimal horizontal compressive stresses. These stresses are sensitive to compressional (white arrows) and extensional forces (black arrows) shown in Figure 6a, mainly owing to the temperature-dependent upper mantle heterogeneities. The results reveal northward high compressional forces over the cold-dense-thick lithospheric layer of the Arabian foreland. The minima of the lateral compressional forces, for example, a lateral extension at a depth of 40 km in Figure 6a, are localized around the Black Sea depression and adjacent to the high Lake VA (black arrows in Figure 6a). These regions and the North Arabian Platform to the south are characterized by high lateral and vertical contrasts in stress second invariant, strain rates, temperature, and viscosity fields (dashed white lines in Figures 6a and 7), as imaged in the shallow-cold temperature anomaly along Profile-1 in Figure 6d. According to the results, high strain rates localize in regions where crustal and lithospheric thicknesses vary drastically, and dynamic topography with a ramp (i.e., step) anomaly pattern is shown in Figure 6c. This also defines two boundaries in the southern part of the plateau, which appear to be related to the Bitlis-Zagros suture and fold belt (i.e., foreland fold/thrust belt/Bitlis-Zagros range; Kadinsky-Cade et al., 1981; Uysal et al., 2021), based on high contrasts in temperatures, stress second invariant and strain rate (Figure 6) and viscosity variations (Figure 7).

**Figure 4.** The 3D thermomechanical numerical modeling results. (a) Dynamic topography-DT (with zero contour line) and 3D convection vectors. (b) Cold upper mantle structures (for simplification of the figure blue iso-contour shows 1100 K between the range of 100–600 km depth) with vectors for the depth of 600 km (cross-section shows temperature variations along Profil-2, Uluocak et al., 2021). Green lines highlight major boundaries and anomalies, that is, the Van Anomaly VA that is located around Lake Van (maximum water depth of 450 m at an altitude of ∼1,650 m), the largest and deepest lake in Turkey (Cukur et al., 2017). LC-Lesser Caucasus. The 3D vectors ($V_{xyz} = (V_x, V_y, V_z)$ in Cartesian coordinates) are scaled by their magnitudes in all figures. Colors of vectors are shown based on vertical components (Velocity-Z indicates $V_z$) in (a) and amplitudes ($|V_{xyz}|$) in (b).
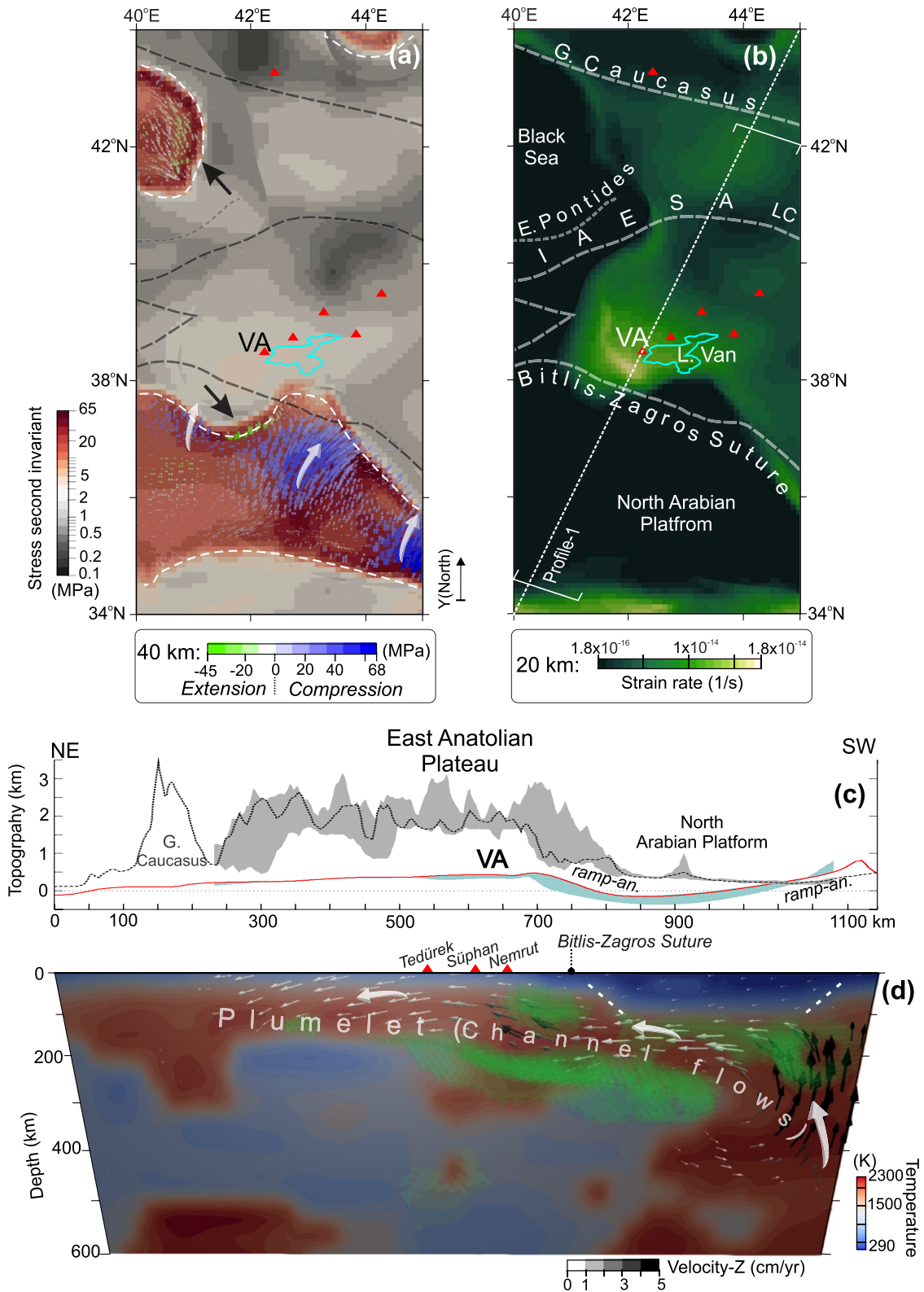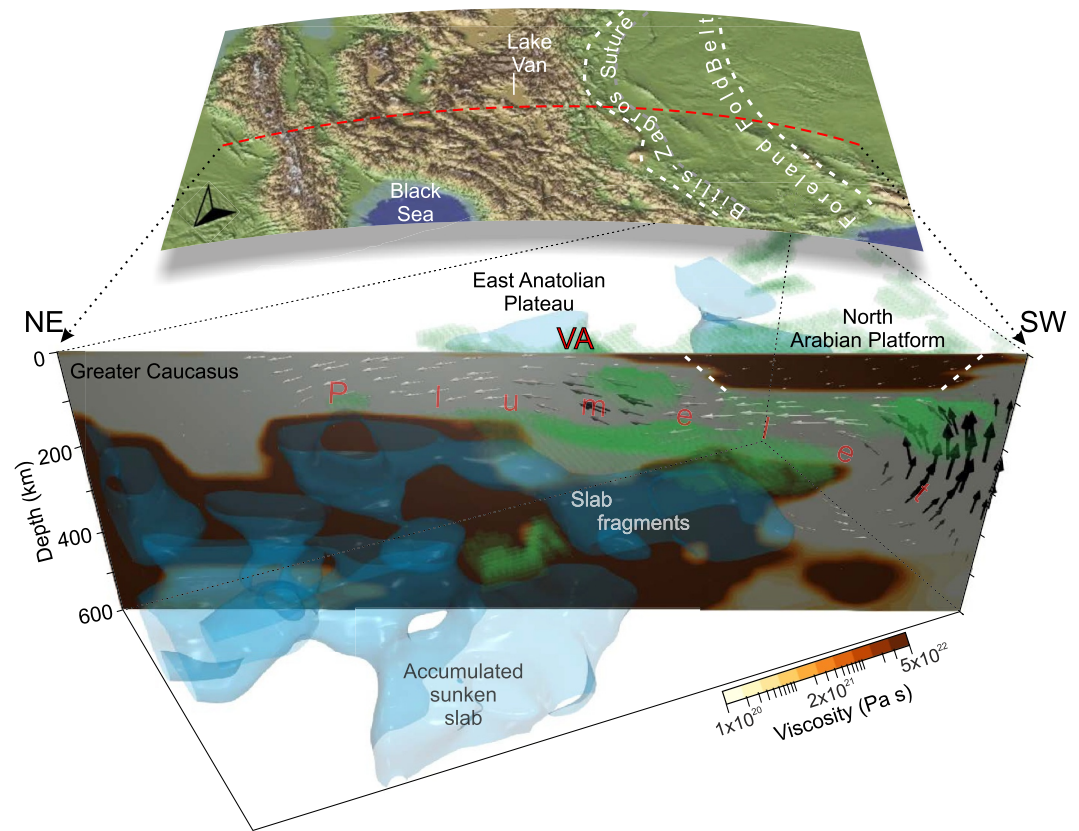
Figure 6.

**Figure 7.** The plumelet with quantified upper mantle structures from the Arabian foreland to the Greater Caucasus. Cross-section of viscosity variations with mantle flows along Profile 1. Iso-contours image cold and dense structures (blue, 1100 K) and high strain rates (green, $\geq 1.5 \times 10^{-4}$ 1/s) under the region. The local upwelling beneath the young volcanoes drives localized dynamic topography (VA-Van anomaly) and the magma-rich intraplate rifting in the extensional Lake Van region. The top panel shows topographic relief with Profile-1 (red line). Dashed white lines correspond to boundaries associated with prominent changes in thicknesses, temperature, viscosity, stress, and strain anomalies in the results (see Figure 6 for colorbar of the vector field).

At long wavelengths, flow vectors related to the upper mantle low-velocity zone extending from the Arabian Platform to the Greater Caucasus (Faccenna et al., 2013; Piromallo & Morelli, 2003; Uluocak et al., 2021) delineate the presence of a plumelet beneath the plateau (the 3D flows in Figure 4b and cross-sections in Figures 6d and 7). This plumelet, involving an injection of mantle flow through a SW-NE lithospheric channel under the plateau is driving local tectonics in eastern Anatolia. Results indicate that interaction between plumelet, moving along the high temperature-low viscosity channel, and cold structures is associated with high strain rates at shallow depths (e.g., down to 300 km in Figures 6d and 7).

## 5. Discussion

Our integrated analyses from instantaneous modeling and observations indicate that plumelet flow through a SW-NE lithospheric channel plays an important role in the tectonics of the Eastern Anatolian Plateau. This flow is in good agreement with previous studies suggesting an active mantle upwelling beneath Anatolia (e.g., Ershov &

---

**Figure 6.** Upper mantle heterogeneities and their surface implications. (a) Horizontal slice showing the second invariant of the deviatoric stress at 40 km depth on a logarithmic scale. The vector field shows the maximum horizontal compressional stress along the north direction ($Y$-axis). (b) Strain rates at 20 km depth-slice. (c) Profile-1 observed (black line) and dynamic topography (DT-red line) with swath profile (shaded areas) for the area shown in (b). (d) Temperature field with a plumelet (channel flow) along Profile-1. Green iso-contour shows high strain rates ($\geq 1.5 \times 10^{-4}$ 1/s) in the upper mantle. Major volcanoes projected onto Profile-1 (G-Greater, VA-Van Anomaly, an.-anomaly). Note that vectors in (d) and are scaled in color by vertical velocity components. Dashed white lines indicate areas where stress, strain, and temperature variations change drastically.

Nikishin, 2004; Faccenna et al., 2013; McNab et al., 2018; Nikogosian et al., 2018; Sharkov et al., 2015; Wilson et al., 2014). The plumelet is consistent with the SW-NE oriented seismic-wave fast axis polarization, recently termed Anatolian Background Splitting (ABS, Lynner et al., 2022), estimated from shear wave splitting anisotropy observations (Lemnifi et al., 2017; Merry et al., 2021 and references therein). Our plumelet result is also supported by large-scale low-speed seismic anomalies extending to the south with an ∼SSW-NNE trending seismic anisotropy pattern (i.e., Dead Sea zone; Merry et al., 2021; Figure 1b; Arvin et al., 2021; Civiero et al., 2022, 2023; Gao et al., 2010; Kaviani et al., 2021; Paul et al., 2014; Qaysi et al., 2018). Moreover, we claim that large-scale numerical geodynamic models (Faccenna et al., 2013), plate-tectonic reconstruction studies (e.g., Gürer & van Hinsbergen, 2019), general characteristics of geochemical data, and spatiotemporal variations of volcanism from the North Arabian Platform to the Greater Caucasus (e.g., Chang & Van der Lee, 2011; Civiero et al., 2022; Ershov & Nikishin, 2004; Faccenna et al., 2013; Hua et al., 2023; Wilson et al., 2014) support our numerical result. As such, the SW-NE-directed plumelet and the associated long-wavelength dynamic support could more likely be linked to the large-scale mantle circulation under the East Anatolian Plateau than the relatively small-scale deformation that might result from subduction-related return flows and/or slab fragmentation reported in many plate boundaries (Faccenna et al., 2010).

It should be noted that there are studies suggesting that a plume (especially in the sense of the typical plume with a mushroom head and/or a plume once fed by deep sources) does not need to be included to explain the presence of anomalously slow/hot structures observed under the plateau and surroundings and petrogenesis of magmas during the collision between Arabian and Eurasian plates (e.g., Keskin, 2007; Koulakov, 2011; Koulakov et al., 2012, 2016; Lustrino & Wilson, 2007; Skobeltsyn et al., 2014 and references therein Memiş et al., 2020; Yang & Faccenda, 2020). In contrast to other regions where plume-related extensional tectonics and dynamic uplift are invoked (e.g., High Atlas of Morocco; Lanari et al., 2023), in Anatolia the role of thermal perturbation of the metasomatized subcontinental lithosphere and indentation tectonics and/or lithospheric delamination with crustal heating and thinning (Figure 2) have been prominent hypotheses for the high plateau and magmatism (see Section 2). Besides, both asthenospheric and lithospheric mantle sources of the post-collisional magmatism (≤6 Ma) are documented specifically in the plateau (Aclan et al., 2020; Oyan et al., 2023 and references therein). However, due to the multicomponent mixing of magma in the collisional zones (e.g., Lustrino et al., 2012; Oyan et al., 2016), the trace element geochemistry and isotope signature of the mantle source can be complicated in terms of interpretation of the plume-induced melting in many areas, such as East African Rift volcanism, where low isotope ratios are documented in lavas and mantle xenoliths (Brune et al., 2023 and references therein). Thus, it can be stated that active plumes in different evolutionary processes and intraplume heterogeneities can have complex signatures in collision zones (e.g., Meshesha & Shinjo, 2008). Also, the possible location of plume source(s), the plume-migration channel, and even the number of plumes beneath East Africa and Arabia are controversial (e.g., Agostini et al., 2021 and references therein) mainly owing to differences in seismic tomography models and their interpretations. Yet, the recent seismic waveform tomography data together with anisotropy models in the African-Arabian region offer possible sources that might feed seemingly connected plume heads and hence may influence the East Anatolian Plateau (Civiero et al., 2022 and references therein) unlike interpretations suggesting a common mantle reservoir in response to Super African Plume migration (e.g., caused by pressure-driven lateral traveling from the Afar hot spot to Anatolia, over ∼2,500 km in 11 Myrs, Hua et al., 2023). That is, upper mantle slow velocities that are localized beneath Kenya, Afar, and Levant regions (at a depth of ≥∼330 km) and interconnected sub-lithospheric slow seismic anomalies can be interpreted as plume sources and heads, respectively (Civiero et al., 2022). We, therefore, suggest that the presence of the aforementioned large-scale (e.g., Figure 1b) and regional (e.g., EAS in Figure 3) low/ultralow seismic anomalies (also hot upper mantle anomalies in e.g., Figures 4b and 6) cannot easily be accounted for by compressional forces alone or by wholesale delamination of the Neotethyan lithospheric mantle. A plumelet, as identified here, best accounts for the seismic anomalies across this region from the Arabian platform to the Greater Caucasus.

A plumelet hypothesis also best explains the mantle melt source domains inferred from the petrological and geochemical characteristics of erupted products at the surface, that is, in the Dead Sea Fault zone, Karacadağ volcanics in the Arabian foreland and across the Arabian-Caucasus region (Agostini et al., 2021; Faccenna et al., 2013; Hua et al., 2023; Keskin et al., 2012; Nikogosian et al., 2018; Rabayrol et al., 2019; Sharkov et al., 2015). The high variability in the composition of the young magmatism at such a short distance in the plateau may be an indicator of a patchy pattern of uppermost mantle structures (e.g., Artemieva &

Shulgin, 2019) with or without relaminated shallow lithospheric mantle (∼5–11 km thickening in the lithospheric layer from ∼6 Ma to 1 Ma following the delamination at ∼5–6 Ma; Oyan et al., 2023) or complex processes of lithospheric removal mechanism (e.g., fragmentation/piecemeal detachment).

We propose a shallow-regional mantle upwelling into the lithospheric gap that generates a localized positive dynamic topography (∼500 m) around Lake Van (VA-Van Anomaly, Figure 4a). In other words, dynamic support caused by localized upper mantle flows with increasing vertical amplitudes (Figures 5 and 6d) explains extensional tectonics in the plateau, in the Lake Van region, under a compressional regime. This result is consistent with the interpretation that Lake Van, one of the largest soda water lakes on the earth, was formed by extensional tectonics leading to the graben and half-graben structures during the past ∼600 ka (Cukur et al., 2017). While ongoing compression is documented in and around the lake, young rapid uplift (∼14 ka) accompanied by erosion is also interpreted from the seismic reflection studies in Lake Van and its sub-basins (Cukur et al., 2017). It is also inferred from paleo-salinity and -elevation studies that tectono-magmatic activities continue under the lake (Cukur et al., 2015; Toker et al., 2017; Tomonaga et al., 2014 and references therein). That is, the Lake Van zone with its (a) local kinematics (e.g., N-S striking normal faulting, Toker, 2006); (b) anomalously low subcrustal seismic velocities; (c) partially melted-thinnest crust (∼40 km, Özacar et al., 2008; Toker, 2006; Zhu, 2018); (d) regional decreases in the density contrast between crust and mantle (Karabulut et al., 2019); (e) young volcanoes (≤6 Ma, Rabayrol et al., 2019; Schleiffarth et al., 2018); (f) young uplift pattern (e.g., domed-like uplift ∼500 m from river inversion studies, Molin et al., 2023) can be attributed to a convective-induced extensional tectonic regime (e.g., Alkan et al., 2020; Selçuk et al., 2020; Uluocak et al., 2021). Thus, considering the mantle-induced heating and the localization of high stress and strain rates (Figure 6) with velocity vectors (e.g., Figures 4 and 7), this region might be the weakest part of the plateau, where multiple forces are active in the form of extensional faulting and rifting in the collisional zone (e.g., triple junction caused by horizontal and vertical displacements). Besides, the location of the youngest volcano (i.e., the rift volcano of Nemrut) and its alkaline to peralkaline magma contents (Cukur et al., 2017 and references therein) support our results implying active intraplate rift tectonics here.

Our results also reveal prominent lithospheric boundaries in the south, as shown in Figure 7. It should be noted that the specific tectonic boundaries estimated from the numerical model do not necessarily match precisely with the observed discrete tectonic features, for example, in the case of the geometry of the Bitlis-Zagros Suture zone (Figure 7). Interpretation of a crustal suture as an indicator of a former lithospheric boundary could be subjective (e.g., Okay & Tüysüz, 1999), especially in such regions of considerable tectonic shortening and deformation. Further, studies have shown that pre-existing structures in the lithosphere can be the primary control on crustal deformation regardless of the underlying mantle dynamics (Heron et al., 2016, 2019). Thus, pre-existing features of the lithosphere—which could have accumulated through the long history of Tethyan tectonics—may likely be the main control on the geometry of a surface feature like the Bitlis-Zagros suture.

All in all, our results from the model and analyses may reconcile the different processes proposed so far in the East Anatolian Plateau, as mantle flow - plumelet - may well have triggered and sustained upper mantle deformations. That is, we suggest that the plumelet, which was strengthened after the removal of the subducted Neotethyan slab, became the engine of the most recent vertical and horizontal mantle forcings, contributing to large-scale plate tectonics and surface deflection. At short wavelengths, we show a plumelet-provoked regional upwelling under the plateau (e.g., Figures 5, 6d, and 7), which drives the magma-rich Lake Van rift tectonics. It has been documented that once the lithosphere breaks, the evolution of rift zones can be highly variable over time due to forces that reactivate inherited weaknesses (Brune et al., 2023 and references therein). In addition to other forces that may yield the strength of the stable lithosphere (e.g., steady-state small-scale convection flows in the collisional regions, Jolivet et al., 2016 and references therein), Neotethyan subduction itself may accelerate the tensional stress owing to the large density and temperature contrasts becoming the major driving force for the intracontinental rift zones (pull and/or roll back, e.g., Brune et al., 2023; Merle, 2011). Temporal variations of these complex deformations may need further explanations; however, we suggest active rifting in the East Anatolian Plateau based on our thermomechanical modeling results.

## 6. Conclusion

We investigate mantle dynamics in the East Anatolian Plateau (Figure 1), one of the most intriguing segments of the Arabian-Eurasian continental collision zone, with its records of both subduction- and post-subduction-related deformations. Based on our results, we propose that a prominent SW-NE-oriented mantle flow—a plumelet—is traveling through a lithospheric channel beneath eastern Anatolia from the Arabian foreland to the Greater Caucasus (Figure 4). The plumelet-provoked forces have an important role in the post-subduction tectonics in the region, favoring NE compression with long-wavelength convective support (∼400 m) on topography and westward escape of the Anatolian plate.

We show the localized and linearized stress and strain anomalies as an expression of compressive or tensional forces (Figure 6), which can be important sources of intraplate deformations (e.g., Brune et al., 2023). According to the results, high contrasts in stress, strain, temperature, and viscosity variations (Figure 7) correspond to the Bitlis-Zagros suture and fold belt in the south of the plateau. Zones with high strain ratios at relatively shallow depths (≤300 km, Figures 6a and 6d) reveal the interaction between the plumelet and shallow cold structures by indicating an active deformation (i.e., thermally eroded zone) beneath the region.

We interpret localized extensional forces and dynamic support in the Lake Van region by relating them to the small-scale convection pattern beneath this part of the plateau. Based on our analysis, we contend that the magma-rich Lake Van rifting in the Africa-Arabia-Anatolian plume-rift system may have occurred after processes initiated by the subduction-related forces and sustained by a plumelet. Moreover, because of the dynamic interactions between upper mantle forces, rifting in continental collisional settings can be a cross-scale process that never reaches a final rift maturity compared to, for instance, a nascent plate boundary with perfectly symmetric upwelling divergent flows and their surface implications.

## Appendix A: Reference Parameters for the Numerical Model

Reference parameters used in the 3D instantaneous (present-day) geodynamic model are shown in Table A1.

**Table A1**
*Parameters Used in the Experiment (Naliboff & Buiter, 2015; Ranalli, 1995; Uluocak et al., 2021 and References Therein)*

| Mechanical parameters | Crust (wet quartz) | Mantle lithosphere (dry olivine) | Asthenospheric mantle (dry olivine) |
|---|---|---|---|
| Density (kg m$^{-3}$) $\rho_0$ | 2,840 | 3,300 | 3,260 |
| Viscosity pre-factor ($B$; Pa$^{-n}$ s$^{-1}$) | $8.57 \times 10^{-28}$ | $6.52 \times 10^{-16}$ | $6.52 \times 10^{-16}$ |
| Power law (stress exponent) ($n$) | 4 | 3.5 | 3.5 |
| Activation energy ($Q$; kJ mol$^{-1}$) | 223 | 530 | 530 |
| Thermal conductivity ($k$; WmK) | 2.5 | 2.25 | 2.25 |

*Note.* The internal friction angle ($\varphi$) = 20° and the specific heat capacity ($C_p$) = 750 (J kg$^{-1}$ K$^{-1}$) for all materials. Activation volumes ($V$) = $18 \times 10^{-6}$ (m$^3$ mol$^{-1}$) for the materials beneath the crust. The reference strain rate = $1 \times 10^{-14}$ s$^{-1}$, the viscosity limits are $\eta_e = 1 \times 10^{20}$–$5 \times 10^{22}$ Pa s (e.g., Uluocak et al., 2021 and references therein).

## Conflict of Interest

The authors declare no conflicts of interest relevant to this study.

## Data Availability Statement

The free-air gravity and topography data were constructed using the Earth Gravitational Model 2012 (Bonvalot et al., 2012; https://bgi.obs-mip.fr/catalogue/?uuid=df2dab2d-a826-4776-b49f-61e8b284c409). All model data sets corresponding to codes and input and output data that were used to create results and figures are given on

Uluocak (2024). Feel free to contact the corresponding author (Ebru Şengül Uluocak), who is an open-source advocate and a supporter of open-science, for the archive of data sets.

# References

Aclan, M., Oyan, V., & Köse, O. (2020). Petrogenesis and the evolution of Pliocene Timar basalts in the east of Lake Van, Eastern Anatolia, Turkey: A consequence of the partial melting of a metasomatized spinel–rich lithospheric mantle source. *Journal of African Earth Sciences*, *168*, 103844. https://doi.org/10.1016/j.jafrearsci.2020.103844

Agostini, S., Di Giuseppe, P., Manetti, P., Doglioni, C., & Conticelli, S. (2021). A heterogeneous subcontinental mantle under the African–Arabian Plate boundary revealed by boron and radiogenic isotopes. *Scientific Reports*, *11*(1), 11230. https://doi.org/10.1038/s41598-021-90275-7

Ahrens, J., Geveci, B., Law, C., Hansen, C., & Johnson, C. (2005). ParaView: An end-user tool for large data visualization, *The visualization handbook* (pp. 717–731). https://doi.org/10.1016/b978-012387582-2/50038-1

Alkan, H., Çınar, H., & Oreshin, S. (2020). Lake Van (Southeastern Turkey) experiment: Receiver function analyses of lithospheric structure from teleseismic observations. *Pure and Applied Geophysics*, *177*(8), 3891–3909. https://doi.org/10.1007/s00024-020-02447-7

Artemieva, I. M., & Shulgin, A. (2019). Geodynamics of Anatolia: Lithosphere thermal structure and thickness. *Tectonics*, *38*(12), 4465–4487. https://doi.org/10.1029/2019tc005594

Arvin, S., Sobouti, F., Priestley, K., Ghods, A., Motaghi, K., Tilmann, F., & Eken, T. (2021). Seismic anisotropy and mantle deformation in NW Iran inferred from splitting measurements of SK (K) S and direct S phases. *Geophysical Journal International*, *226*(2), 1417–1431. https://doi.org/10.1093/gji/ggab181

Ayachit, U. (2015). *The paraview guide: A parallel visualization application*. Kitware, Inc.

Bangerth, W., Dannberg, J., Fraters, M., Gassmoeller, R., Glerum, A., Timo Heister, T., et al. (2022). *ASPECT v2.4.0*. Zenodo. https://doi.org/10.5281/zenodo.6903424

Bangerth, W., Dannberg, J., Gassmoeller, R., & Timo Heister, T. (2019). *ASPECT v2.1.0*. Zenodo. https://doi.org/10.5281/zenodo.2653531

Barazangi, M., Sandvol, E., & Seber, D. (2006). Structure and tectonic evolution of the Anatolian plateau in eastern Turkey. In Y. Dilek & S. Pavlides (Eds.), *Postcollisional tectonics and magmatism in the Mediterranean region and Asia* (Vol. 409, pp. 463–474). Geological Society of America Special Paper. https://doi.org/10.1130/2006.2409(22)

Bartol, J., & Govers, R. (2014). A single cause for uplift of the Central and Eastern Anatolian plateau? *Tectonophysics*, *637*, 116–136. https://doi.org/10.1016/j.tecto.2014.10.002

Becker, T. W., & Boschi, L. (2002). A comparison of tomographic and geodynamic mantle models. *Geochemistry, Geophysics, Geosystems*, *3*(1), 1003. https://doi.org/10.1029/2001GC000168

Black, B. A., Karlstrom, L., & Mather, T. A. (2021). The life cycle of large igneous provinces. *Nature Reviews Earth & Environment*, *2*(12), 840–857. https://doi.org/10.1038/s43017-021-00221-4

Bonvalot, S., Balmino, G., Briais, A., Kuhn, M., Peyrefitte, A., Vales, N., et al. (2012). *Commission for the geological map of the world*. BGI-CGMW-CNES-IRD.

Brune, S., Kolawole, F., Olive, J. A., Stamps, D. S., Buck, W. R., Buiter, S. J., et al. (2023). Geodynamics of continental rift initiation and evolution. *Nature Reviews Earth & Environment*, *4*(4), 235–253. https://doi.org/10.1038/s43017-023-00391-3

Burov, E., & Gerya, T. (2014). Asymmetric three-dimensional topography over mantle plumes. *Nature*, *513*(7516), 85–89. https://doi.org/10.1038/nature13703

Burov, E., & Guillou-Frottier, L. (2005). The plume head–continental lithosphere interaction using a tectonically realistic formulation for the lithosphere. *Geophysical Journal International*, *161*(2), 469–490. https://doi.org/10.1111/j.1365-246x.2005.02588.x

Campbell, I. H., & Griffiths, R. W. (1990). Implications of mantle plume structure for the evolution of flood basalts. *Earth and Planetary Science Letters*, *99*(1–2), 79–93. https://doi.org/10.1016/j.epsl.2016.05.006

Capitanio, F. A. (2016). The role of the Miocene-to-Pliocene transition in the Eastern Mediterranean extrusion tectonics: Constraints from numerical modelling. *Earth and Planetary Science Letters*, *448*, 122–132. https://doi.org/10.1016/j.epsl.2016.05.006

Chang, S. J., & Van der Lee, S. (2011). Mantle plumes and associated flow beneath Arabia and East Africa. *Earth and Planetary Science Letters*, *302*(3–4), 448–454. https://doi.org/10.1016/j.epsl.2010.12.050

Civiero, C., Armitage, J. J., Goes, S., & Hammond, J. O. (2019). The seismic signature of upper-mantle plumes: Application to the Northern East African Rift. *Geochemistry, Geophysics, Geosystems*, *20*(12), 6106–6122. https://doi.org/10.1029/2019gc008636

Civiero, C., Celli, N. L., & Tesauro, M. (2023). Revisiting the geodynamics of the Middle East region from an integrated geophysical perspective. *Journal of Geodynamics*, *158*, 102005. https://doi.org/10.1016/j.jog.2023.102005

Civiero, C., Lebedev, S., & Celli, N. L. (2022). A complex mantle plume head below East Africa-Arabia shaped by the lithosphere-asthenosphere boundary topography. *Geochemistry, Geophysics, Geosystems*, *23*(11), e2022GC010610. https://doi.org/10.1029/2022GC010610

Clevenger, T. C., & Heister, T. (2021). Comparison between algebraic and matrix-free geometric multigrid for a Stokes problem on adaptive meshes with variable viscosity. *Numerical Linear Algebra with Applications*, *28*(5), e2375. https://doi.org/10.1002/nla.2375

Cowgill, E., Forte, A. M., Niemi, N., Avdeev, B., Tye, A., Trexler, C., et al. (2016). Relict basin closure and crustal shortening budgets during continental collision: An example from Caucasus sediment provenance. *Tectonics*, *35*(12), 2918–2947. https://doi.org/10.1002/2016tc004295

Cukur, D., Krastel, S., Çağatay, M. N., Damcı, E., Meydan, A. F., & Kim, S. P. (2015). Evidence of extensive carbonate mounds and sublacustrine channels in shallow waters of Lake Van, eastern Turkey, based on high-resolution chirp subbottom profiler and multibeam echosounder data. *Geo-Marine Letters*, *35*(5), 329–340. https://doi.org/10.1007/s00367-015-0410-x

Cukur, D., Krastel, S., Tomonaga, Y., Schmincke, H. U., Sumita, M., Meydan, A. F., et al. (2017). Structural characteristics of the Lake Van Basin, eastern Turkey, from high-resolution seismic reflection profiles and multibeam echosounder data: Geologic and tectonic implications. *International Journal of Earth Sciences*, *106*(1), 239–253. https://doi.org/10.1007/s00531-016-1312-5

Dannberg, J., & Sobolev, S. V. (2015). Low-buoyancy thermochemical plumes resolve controversy of classical mantle plume concept. *Nature Communications*, *6*(1), 6960. https://doi.org/10.1038/ncomms7960

Daradich, A., Mitrovica, J. X., Pysklywec, R. N., Willett, S. D., & Forte, A. M. (2003). Mantle flow, dynamic topography, and rift-flank uplift of Arabia. *Geology*, *31*(10), 901–904. https://doi.org/10.1130/g19661.1

Demir, T., Seyrek, A., Guillou, H., Scaillet, S., Westaway, R., & Bridgland, D. (2009). Preservation by basalt of a staircase of latest Pliocene terraces of the River Murat in eastern Turkey: Evidence for rapid uplift of the eastern Anatolian Plateau. *Global and Planetary Change*, *68*(4), 254–269. https://doi.org/10.1016/j.gloplacha.2009.02.008

Dilek, Y., & Sandvol, E. (2006). Collision tectonics of the Mediterranean region: Causes and consequences. In Y. Dilek & S. Pavlides (Eds.), *Postcollisional tectonics and magmatism in the Mediterranean region and Asia* (Vol. 409, pp. 1–13). Geological Society of America Special Paper.

Elitok, Ö., & Dolmaz, M. N. (2008). Mantle flow-induced crustal thinning in the area between the easternmost part of the Anatolian plate and the Arabian Foreland (E Turkey) deduced from the geological and geophysical data. *Gondwana Research*, *13*(3), 302–318. https://doi.org/10.1016/j.gr.2007.08.007

Emre, Ö., Duman, T. Y., Özalp, S., Şaroğlu, F., Olgun, Ş., Elmacı, H., & Çan, T. (2018). Active fault database of Turkey. *Bulletin of Earthquake Engineering*, *16*(8), 3229–3275. https://doi.org/10.1007/s10518-016-0041-2

England, P., Houseman, G., & Nocquet, J. M. (2016). Constraints from GPS measurements on the dynamics of deformation in Anatolia and the Aegean. *Journal of Geophysical Research: Solid Earth*, *121*(12), 8888–8916. https://doi.org/10.1002/2016JB013382

England, P., & McKenzie, D. (1982). A thin viscous sheet model for continental deformation. *Geophysical Journal International*, *70*(2), 295–321. https://doi.org/10.1111/j.1365-246x.1982.tb04969.x

Ershov, A. V., & Nikishin, A. M. (2004). Recent geodynamics of the Caucasus–Arabia–East Africa region. *Geotectonics*, *38*(2), 123–136.

Faccenna, C., & Becker, T. W. (2010). Shaping mobile belts by small-scale convection. *Nature*, *465*(7298), 602–605. https://doi.org/10.1038/nature09064

Faccenna, C., & Becker, T. W. (2020). Topographic expressions of mantle dynamics in the Mediterranean. *Earth-Science Reviews*, *209*, 103327. https://doi.org/10.1016/j.earscirev.2020.103327

Faccenna, C., Becker, T. W., Auer, L., Billi, A., Boschi, L., Brun, J. P., et al. (2014). Mantle dynamics in the Mediterranean. *Reviews of Geophysics*, *52*(3), 283–332. https://doi.org/10.1002/2013RG000444

Faccenna, C., Becker, T. W., Jolivet, L., & Keskin, M. (2013). Mantle convection in the Middle East: Reconciling Afar upwelling, Arabia indentation and Aegean trench rollback. *Earth and Planetary Science Letters*, *375*, 254–269. https://doi.org/10.1016/j.epsl.2013.05.043i

Faccenna, C., Becker, T. W., Lallemand, S., Lagabrielle, Y., Funiciello, F., & Piromallo, C. (2010). Subduction-triggered magmatic pulses: A new class of plumes? *Earth and Planetary Science Letters*, *299*(1–2), 54–68. https://doi.org/10.1016/j.epsl.2010.08.012

Faccenna, C., Bellier, O., Martinod, J., Piromallo, C., & Regard, V. (2006). Slab detachment beneath eastern Anatolia: A possible cause for the formation of the North Anatolian fault. *Earth and Planetary Science Letters*, *242*(1–2), 85–97. https://doi.org/10.1016/j.epsl.2005.11.046

Fichtner, A., Trampert, J., Cupillard, P., Saygin, E., Taymaz, T., Capdeville, Y., & Villasenor, A. (2013). Multiscale full waveform inversion. *Geophysical Journal International*, *194*(1), 534–556. https://doi.org/10.1093/gji/ggt118

Fraters, M. R., Bangerth, W., Thieulot, C., Glerum, A. C., & Spakman, W. (2019). Efficient and practical Newton solvers for non-linear Stokes systems in geodynamic problems. *Geophysical Journal International*, *218*(2), 873–894. https://doi.org/10.1093/gji/ggz183

Gao, S. S., Liu, K. H., & Abdelsalam, M. G. (2010). Seismic anisotropy beneath the Afar Depression and adjacent areas: Implications for mantle flow. *Journal of Geophysical Research*, *115*(B12), B12330. https://doi.org/10.1029/2009JB007141

Glerum, A., Thieulot, C., Fraters, M., Blom, C., & Spakman, W. (2018). Nonlinear viscoplasticity in ASPECT: Benchmarking and applications to subduction. *Solid Earth*, *9*(2), 267–294. https://doi.org/10.5194/se-9-267-2018

Göğüş, O. H., & Pysklywec, R. N. (2008). Mantle lithosphere delamination driving plateau uplift and synconvergent extension in eastern Anatolia. *Geology*, *36*(9), 723–726. https://doi.org/10.1130/g24982a.1

Gürer, D., & van Hinsbergen, D. J. (2019). Diachronous demise of the Neotethys Ocean as a driver for non-cylindrical orogenesis in Anatolia. *Tectonophysics*, *760*, 95–106. https://doi.org/10.1016/j.tecto.2018.06.005

Hassan, R., Williams, S. E., Gurnis, M., & Müller, D. (2020). East African topography and volcanism explained by a single, migrating plume. *Geoscience Frontiers*, *11*(5), 1669–1680. https://doi.org/10.1016/j.gsf.2020.01.003

Heister, T., Dannberg, J., Gassmöller, R., & Bangerth, W. (2017). High accuracy mantle convection simulation through modern numerical methods–II: Realistic models and problems. *Geophysical Journal International*, *210*(2), 833–851. https://doi.org/10.1093/gji/ggx195

Heron, P. J., Pysklywec, R. N., & Stephenson, R. (2016). Lasting mantle scars lead to perennial plate tectonics. *Nature Communications*, *7*(1), 11834. https://doi.org/10.1038/ncomms11834

Heron, P. J., Pysklywec, R. N., Stephenson, R., & Van Hunen, J. (2019). Deformation driven by deep and distant structures: Influence of a mantle lithosphere suture in the Ouachita orogeny, southeastern United States. *Geology*, *47*(2), 147–150. https://doi.org/10.1130/g45690.1

Hua, J., Fischer, K. M., Gazel, E., Parmentier, E. M., & Hirth, G. (2023). Long-distance asthenospheric transport of plume-influenced mantle from Afar to Anatolia. *Geochemistry, Geophysics, Geosystems*, *24*(2), e2022GC010605. https://doi.org/10.1029/2022gc010605

Ihinger, P. D. (1995). Mantle flow beneath the Pacific Plate; evidence from seamount segments in the Hawaiian-Emperor Chain. *American Journal of Science*, *295*(9), 1035–1057. https://doi.org/10.2475/ajs.295.9.1035

Jolivet, L., Faccenna, C., Agard, P., Frizon de Lamotte, D., Menant, A., Sternai, P., & Guillocheau, F. (2016). Neo-Tethys geodynamics and mantle convection: From extension to compression in Africa and a conceptual model for obduction. *Canadian Journal of Earth Sciences*, *53*(11), 1190–1204. https://doi.org/10.1139/cjes-2015-0118

Jolivet, L., Menant, A., Sternai, P., Rabillard, A., Arbaret, L., Augier, R., et al. (2015). The geological signature of a slab tear below the Aegean. *Tectonophysics*, *659*, 166–182. https://doi.org/10.1016/j.tecto.2015.08.004

Kaban, M. K., Petrunin, A. G., El Khrepy, S., & Al-Arifi, N. (2018). Diverse continental subduction scenarios along the Arabia-Eurasia collision zone. *Geophysical Research Letters*, *45*(14), 6898–6906. https://doi.org/10.1029/2018gl078074

Kadinsky-Cade, K., Barazangi, M., Oliver, J., & Isacks, B. (1981). Lateral variations of high-frequency seismic wave propagation at regional distances across the Turkish and Iranian plateaus. *Journal of Geophysical Research*, *86*(B10), 9377–9396. https://doi.org/10.1029/jb086ib10p09377

Karabulut, H., Paul, A., Özbakır, A. D., Ergün, T., & Şentürk, S. (2019). A new crustal model of the Anatolia–Aegean domain: Evidence for the dominant role of isostasy in the support of the Anatolian plateau. *Geophysical Journal International*, *218*(1), 57–73. https://doi.org/10.1093/gji/ggz147

Karato, S. I. (1993). Importance of anelasticity in the interpretation of seismic tomography. *Geophysical Research Letters*, *20*(15), 1623–1626. https://doi.org/10.1029/93gl01767

Kaviani, A., Mahmoodabadi, M., Rümpker, G., Pilia, S., Tatar, M., Nilforoushan, F., et al. (2021). Mantle-flow diversion beneath the Iranian plateau induced by Zagros' lithospheric keel. *Scientific Reports*, *11*(1), 2848. https://doi.org/10.1038/s41598-021-81541-9

Keskin, M. (2003). Magma generation by slab steepening and breakoff beneath a subduction-accretion complex: An alternative model for collision-related volcanism in Eastern Anatolia, Turkey. *Geophysical Research Letters*, *30*(24), 8046. https://doi.org/10.1029/2003GL018019

Keskin, M. (2007). Eastern Anatolia: A hotspot in a collision zone without a mantle plume. *Geological Society of America Special Paper*, *430*(32), 693–722. https://doi.org/10.1130/2007.2430

Keskin, M., Chugaev, A. V., Lebedev, V. A., Sharkov, E. V., Oyan, V., & Kavak, O. (2012). The geochronology and origin of mantle sources for late Cenozoic intraplate volcanism in the frontal part of the Arabian plate in the Karacadağ neovolcanic area of Turkey. Part 2. The results of

geochemical and isotope (Sr-Nd-Pb) studies. *Journal of Volcanology and Seismology*, *6*, 361–382. https://doi.org/10.1134/s0742046312060048

Keskin, M., Pearce, J. A., & Mitchell, J. G. (1998). Volcano-stratigraphy and geochemistry of collision-related volcanism on the Erzurum–Kars Plateau, northeastern Turkey. *Journal of Volcanology and Geothermal Research*, *85*(1–4), 355–404. https://doi.org/10.1016/s0377-0273(98)00063-8

Komut, T. (2015). High surface topography related to upper mantle flow beneath Eastern Anatolia. *Geophysical Journal International*, *203*(2), 1263–1273. https://doi.org/10.1093/gji/ggv374

Koppers, A. A., Becker, T. W., Jackson, M. G., Konrad, K., Müller, R. D., Romanowicz, B., et al. (2021). Mantle plumes and their role in Earth processes. *Nature Reviews Earth & Environment*, *2*(6), 382–401. https://doi.org/10.1038/s43017-021-00168-6

Koptev, A., Cloetingh, S., & Ehlers, T. A. (2021). Longevity of small-scale ('baby') plumes and their role in lithospheric break-up. *Geophysical Journal International*, *227*(1), 439–471. https://doi.org/10.1093/gji/ggab223

Koulakov, I. (2011). High-frequency P and S velocity anomalies in the upper mantle beneath Asia from inversion of worldwide traveltime data. Journal of Geophysical Research. *Solid Earth*, *116*(B4), B04301. https://doi.org/10.1029/2010JB007938

Koulakov, I., Burov, E., Cloetingh, S., El Khrepy, S., Al-Arifi, N., & Bushenkova, N. (2016). Evidence for anomalous mantle upwelling beneath the Arabian Platform from travel time tomography inversion. *Tectonophysics*, *667*, 176–188. https://doi.org/10.1016/j.tecto.2015.11.022

Koulakov, I., Zabelina, I., Amanatashvili, I., & Meskhia, V. (2012). Nature of orogenesis and volcanism in the Caucasus region based on results of regional tomography. *Solid Earth*, *3*(2), 327–337. https://doi.org/10.5194/se-3-327-2012

Kounoudis, R., Bastow, I. D., Ogden, C. S., Goes, S., Jenkins, J., Grant, B., & Braham, C. (2020). Seismic tomographic imaging of the Eastern Mediterranean mantle: Implications for terminal-stage subduction, the uplift of Anatolia, and the development of the North Anatolian Fault. *Geochemistry, Geophysics, Geosystems*, *21*(7), e2020GC009009. https://doi.org/10.1029/2020gc009009

Kronbichler, M., Heister, T., & Bangerth, W. (2012). High accuracy mantle convection simulation through modern numerical methods. *Geophysical Journal International*, *191*(1), 12–29. https://doi.org/10.1111/j.1365-246X.2012.05609.x

Lanari, R., Faccenna, C., Natali, C., Şengül Uluocak, E., Fellin, M. G., Becker, T. W., et al. (2023). The Atlas of Morocco: A plume-assisted orogeny. *Geochemistry, Geophysics, Geosystems*, *24*(6), e2022GC010843. https://doi.org/10.1029/2022GC010843

Lebedev, V. A., Sharkov, E. V., Keskin, M., & Oyan, V. (2010). Geochronology of the Late Cenozoic volcanism in the area of Van Lake (Turkey): An example of the developmental dynamics for magmatic processes. *Doklady Earth Sciences*, *433*(2), 1031–1037. https://doi.org/10.1134/S1028334X1008009X

Legendre, C. P., Zhao, L., & Tseng, T. L. (2021). Large-scale variation in seismic anisotropy in the crust and upper mantle beneath Anatolia, Turkey. *Communications Earth & Environment*, *2*(1), 73. https://doi.org/10.1038/s43247-021-00142-6

Lei, J., & Zhao, D. (2007). Teleseismic evidence for a break-off subducting slab under Eastern Turkey. *Earth and Planetary Science Letters*, *257*(1–2), 14–28. https://doi.org/10.1016/j.epsl.2007.02.011

Lemnifi, A. A., Elshaafi, A., Karaoğlu, Ö., Salah, M. K., Aouad, N., Reed, C. A., & Yu, Y. (2017). Complex seismic anisotropy and mantle dynamics beneath Turkey. *Journal of Geodynamics*, *112*, 31–45. https://doi.org/10.1016/j.jog.2017.10.004

Lin, C. M., Tseng, T. L., Meliksetian, K., Karakhanyan, A., Huang, B. S., Babayan, H., et al. (2020). Locally thin crust and high crustal $V_p/V_s$ ratio beneath the Armenian Volcanic Highland of the Lesser Caucasus: A case for recent delamination. *Journal of Geophysical Research: Solid Earth*, *125*(9), e2019JB0191510. https://doi.org/10.1029/2019jb019151

Lü, Y., Nir, S., Chen, L., & Chen, Q.-F. (2017). Pn tomography with Moho depth correction from Eastern Europe to western China. *Journal of Geophysical Research: Solid Earth*, *122*(2), 1284–1301. https://doi.org/10.1002/2016JB013052

Lustrino, M., Keskin, M., Mattioli, M., & Kavak, O. (2012). Heterogeneous mantle sources feeding the volcanic activity of Mt. Karacadag (SE Turkey). *Journal of Asian Earth Sciences*, *46*, 120–139. https://doi.org/10.1016/j.jseaes.2011.11.016

Lustrino, M., & Wilson, M. (2007). The circum-Mediterranean anorogenic Cenozoic igneous province. *Earth-Science Reviews*, *81*(1–2), 1–65. https://doi.org/10.1016/j.earscirev.2006.09.002

Lynner, C., Delph, J. R., Portner, D. E., Beck, S. L., Sandvol, E., & Özacar, A. A. (2022). Slab induced mantle upwelling beneath the Anatolian plateau. *Geophysical Research Letters*, *49*(11), e2021GL097451. https://doi.org/10.1029/2021gl097451

Maestrelli, D., Brune, S., Corti, G., Keir, D., Muluneh, A. A., & Sani, F. (2022). Analog and numerical modeling of Rift-Rift-Rift triple junctions. *Tectonics*, *41*(10), e2022TC007491. https://doi.org/10.1029/2022TC007491

McNab, F., Ball, P. W., Hoggard, M. J., & White, N. J. (2018). Neogene uplift and magmatism of Anatolia: Insights from drainage analysis and basaltic geochemistry. *Geochemistry, Geophysics, Geosystems*, *19*(1), 175–213. https://doi.org/10.1002/2017GC007251

Memiş, C., Göğüş, O. H., Uluocak, E. Ş., Pysklywec, R., Keskin, M., Şengör, A. M. C., & Topuz, G. (2020). Long wavelength progressive plateau uplift in Eastern Anatolia since 20 Ma: Implications for the role of slab peel-back and break-off. *Geochemistry, Geophysics, Geosystems*, *21*(2), e2019GC008726. https://doi.org/10.1029/2019GC008726

Merle, O. (2011). A simple continental rift classification. *Tectonophysics*, *513*(1–4), 88–95. https://doi.org/10.1016/j.tecto.2011.10.004

Merry, T., Bastow, I., Kounoudis, R., Ogden, C., Bell, R., Jones, L., et al. (2021). The influence of the North Anatolian Fault and a fragmentingslab architecture on upper mantle seismic anisotropy in the eastern Mediterranean. *Geochemistry, Geophysics, Geosystems*, *22*(9), 1525–2027. https://doi.org/10.1029/2021gc009896

Meshesha, D., & Shinjo, R. (2008). Rethinking geochemical feature of the Afar and Kenya mantle plumes and geodynamic implications. *Journal of Geophysical Research*, *113*(B9), B09209. https://doi.org/10.1029/2007jb005549

Molin, P., Sembroni, A., Ballato, P., & Faccenna, C. (2023). The uplift of an early stage collisional plateau unraveled by fluvial network analysis and river longitudinal profile inversion: The case of the Eastern Anatolian Plateau. *Tectonics*, *42*(8), e2022TC007737. https://doi.org/10.1029/2022tc007737

Naliboff, J., & Buiter, S. J. H. (2015). Rift reactivation and migration during multiphase extension. *Earth and Planetary Science Letters*, *421*, 58–67. https://doi.org/10.1016/j.epsl.2015.03.050

Nikogosian, I. K., Bracco Gartner, A. J., Van Bergen, M. J., Mason, P. R., & Van Hinsbergen, D. J. (2018). Mantle sources of recent Anatolian intraplate magmatism: A regional plume or local tectonic origin? *Tectonics*, *37*(12), 4535–4566. https://doi.org/10.1029/2018tc005219

Okay, A. I., & Tüysüz, O. (1999). Tethyan sutures of northern Turkey. *Geological Society, London, Special Publications*, *156*(1), 475–515. https://doi.org/10.1144/gsl.sp.1999.156.01.22

Okay, A. I., Zattin, M., & Cavazza, W. (2010). Apatite fission-track data for the Miocene Arabia-Eurasia collision. *Geology*, *38*(1), 35–38. https://doi.org/10.1130/g30234.1

Oyan, V., Keskin, M., Lebedev, V. A., Chugaev, A. V., & Sharkov, E. V. (2016). Magmatic evolution of the Early Pliocene Etrüsk stratovolcano, eastern Anatolian collision zone, Turkey. *Lithos*, *256*, 88–108. https://doi.org/10.1016/j.lithos.2016.03.017

Oyan, V., Keskin, M., Lebedev, V. A., Chugaev, A. V., Sharkov, E. V., & Ünal, E. (2017). Petrology and geochemistry of the Quaternary mafic volcanism to the NE of Lake Van, Eastern Anatolian Collision Zone, Turkey. *Journal of Petrology*, *58*(9), 1701–1728. https://doi.org/10.1093/petrology/egx070

Oyan, V., Özdemir, Y., Chugaev, A. V., Oyan, E., & Chernyshev, I. V. (2023). Petrogenesis of Miocene to Quaternary primitive basaltic magmas in the area of Lake Van (East Anatolia, Turkey): A case for relamination of mantle lithosphere after lithospheric delamination. *Contributions to Mineralogy and Petrology*, *178*(12), 88. https://doi.org/10.1007/s00410-023-02070-4

Özacar, A. A., Gilbert, H., & Zandt, G. (2008). Upper mantle discontinuity structure beneath East Anatolian Plateau (Turkey) from receiver functions. *Earth and Planetary Science Letters*, *269*(3–4), 427–435. https://doi.org/10.1016/j.epsl.2008.02.036

Özeren, M. S., & Holt, W. E. (2010). The dynamics of the eastern Mediterranean and eastern Turkey. *Geophysical Journal International*, *183*(3), 1165–1184. https://doi.org/10.1111/j.1365-246X.2010.04819.x

Paul, A., Karabulut, H., Mutlu, A. K., & Salaün, G. (2014). A comprehensive and densely sampled map of shear-wave azimuthal anisotropy in the Aegean-Anatolia region. *Earth and Planetary Science Letters*, *389*, 14–22. https://doi.org/10.1016/j.epsl.2013.12.019

Pearce, J. A., Bender, J. F., De Long, S. E., Kidd, W. S., Low, P. J., Güner, Y., et al. (1990). Genesis of collision volcanism in Eastern Anatolia, Turkey. *Journal of Volcanology and Geothermal Research*, *44*(1–2), 189–229. https://doi.org/10.1016/0377-0273(90)90018-b

Piromallo, C., & Morelli, A. (2003). *P* wave tomography of the mantle under the Alpine–Mediterranean area. *Journal of Geophysical Research*, *108*(B2), 2065. https://doi.org/10.1029/2002JB001757

Portner, D. E., Delph, J. R., Biryol, C. B., Beck, S. L., Zandt, G., Özacar, A. A., et al. (2018). Subduction termination through progressive slab deformation across Eastern Mediterranean subduction zones from updated P-wave tomography beneath Anatolia. *Geosphere*, *14*(3), 907–925. https://doi.org/10.1130/ges01617.1

Priestley, K., & McKenzie, D. (2013). The relationship between shear wave velocity, temperature, attenuation and viscosity in the shallow part of the mantle. *Earth and Planetary Science Letters*, *381*, 78–91. https://doi.org/10.1016/j.epsl.2013.08.022

Pysklywec, R. N., Beaumont, C., & Fullsack, P. (2000). Modeling the behavior of the continental mantle lithosphere during plate convergence. *Geology*, *28*(7), 655–658. https://doi.org/10.1029/2001JB000252

Qaysi, S., Liu, K. H., & Gao, S. S. (2018). A database of shear-wave splitting measurements for the Arabian plate. *Seismological Research Letters*, *89*(6), 2294–2298. https://doi.org/10.1785/0220180144

Rabayrol, F., Hart, C. J. R., & Thorkelson, D. J. (2019). Temporal, spatial, geochemical evolution of late Cenozoic post subduction magmatism in central and eastern Anatolia, Turkey. *Lithos*, *336*, 67–96. https://doi.org/10.1016/j.lithos.2019.03.022

Ranalli, G. (1995). *Rheology of the Earth* (p. 413). Chapman and Hall.

Reid, M. R., Delph, J. R., Cosca, M. A., Schleiffarth, W. K., & Kuşcu, G. G. (2019). Melt equilibration depths as sensors of lithospheric thickness during Eurasia-Arabia collision and the uplift of the Anatolian Plateau. *Geology*, *47*(10), 943–947. https://doi.org/10.1130/G46420.1

Reilinger, R., McClusky, S., Vernant, P., Lawrence, S., Ergintav, S., Cakmak, R., et al. (2006). GPS constraints on continental deformation in the Africa-Arabia-Eurasia continental collision zone and implications for the dynamics of plate interactions. *Journal of Geophysical Research*, *111*(B5), B05411. https://doi.org/10.1029/2005JB004051

Rose, I., Buffett, B., & Heister, T. (2017). Stability and accuracy of free surface time integration in viscous flows. *Physics of the Earth and Planetary Interiors*, *262*, 90–100. https://doi.org/10.1016/j.pepi.2016.11.007

Ryan, W. B. F., Carbotte, S. M., Coplan, J. O., O'Hara, S., Melkonian, A., Arko, R., et al. (2009). Global multi-resolution topography synthesis. *Geochemistry, Geophysics, Geosystems*, *10*(3), Q03014. https://doi.org/10.1029/2008GC002332

Schleiffarth, W., Darin, M., Umhoefer, P., & Reid, R. M. (2018). Dynamics of episodic Late Cretaceous–Cenozoic magmatism across Central to Eastern Anatolia: New insights from an extensive geochronology compilation. *Geosphere*, *14*(5), 1990–2008. https://doi.org/10.1130/GES01647.1

Selçuk, A. S., & Düzgün, M. (2017). Tectonic geomorphology of Başkale Fault zone. *Bulletin of the Mineral Research and Exploration*, *155*(155), 33–46.

Selçuk, A. S., Erturaç, M. K., Sunal, G., & Çakır, Z. (2020). Evaluation of the Plio-Quaternary tectonic stress regime from fault kinematic analysis in the lake Van Basin (Eastern Anatolia). *Journal of Structural Geology*, *140*, 104157. https://doi.org/10.1016/j.jsg.2020.104157

Şengör, A. M. C., & Kidd, W. S. F. (1979). The post–collisional tectonics of the Turkish–Iranian Plateau and a comparison with Tibet. *Tectonophysics*, *55*(3–4), 361–376. https://doi.org/10.1016/0040-1951(79)90184-7

Şengör, A. M. C., Özeren, S., Genç, T., & Zor, E. (2003). East Anatolian high plateau as a mantle-supported, north–south shortened domal structure. *Geophysical Research Letters*, *30*(24), 8045. https://doi.org/10.1029/2003GL017858

Şengör, A. M. C., Özeren, S., Keskin, M., Sakınç, M., Özbakır, A. D., & Kayan, I. (2008). Eastern Turkish high plateau as a small Turkic-type orogen: Implications for post-collisional crust-forming processes in Turkic-type orogens. *Earth-Science Reviews*, *90*(1–2), 1–48. https://doi.org/10.1016/j.earscirev.2008.05.002

Şengör, A. M. C., & Yazıcı, M. (2020). The aetiology of the neotectonic evolution of Turkey. *Mediterranean Geoscience Reviews*, *2*(3), 327–339. https://doi.org/10.1007/s42990-020-00039-0

Şengör, A. M. C., & Yılmaz, Y. (1981). Tethyan evolution of Turkey: A plate tectonic approach. *Tectonophysics*, *75*(3–4), 181–241. https://doi.org/10.1016/0040-1951(81)90275-4

Sharkov, E., Lebedev, V., Chugaev, A., Zabarinskaya, L., Rodnikov, A., Sergeeva, N., & Safonova, I. (2015). The Caucasian-Arabian segment of the Alpine-Himalayan collisional belt: Geology, volcanism and neotectonics. *Geoscience Frontiers*, *6*(4), 513–522. https://doi.org/10.1016/j.gsf.2014.07.001

Shaw, M., & Pysklywec, R. N. (2007). Anomalous uplift of the Apennines and subsidence of the Adriatic: The result of active mantle flow? *Journal of Geophysical Research*, *34*(4), L04311. https://doi.org/10.1029/2006GL028337

Skobeltsyn, G., Mellors, R., Gök, R., Turkelli, N., Yetirmishli, G., & Sandvol, E. (2014). Upper mantle S wave velocity structure of the East Anatolian-Caucasus region. *Tectonics*, *33*(3), 207–221. https://doi.org/10.1002/2013tc003334

Steinberger, B., & O'Connell, R. J. (1998). Advection of plumes in mantle flow: Implications for hotspot motion, mantle viscosity and plume distribution. *Geophysical Journal International*, *132*(2), 412–434. https://doi.org/10.1046/j.1365-246x.1998.00447.x

The MathWorks Inc. (2024). *MATLAB version: 24.1.0.2585741 (R2024a)*. The MathWorks Inc. Retrieved from https://www.mathworks.com

Toker, M. (2006). Van segmenti mikrodeprem potansiyelini kontrol eden neotektonik unsurlar. Toplantısı, Dokuz Eylül Üniversitesi, Jeoloji Mühendisliği Bölümü, Bildiri Özleri Kitabı, Buca, İzmir. *ATAG-10 Aktif Tektonik Araştırma Grubu*, *10*, 91–92. (in Turkish).

Toker, M., Sengor, A. C., Schluter, F. D., Demirbag, E., Cukur, D., Imren, C., & Niessen, F. (2017). The structural elements and tectonics of the Lake Van basin (Eastern Anatolia) from multi-channel seismic reflection profiles. *Journal of African Earth Sciences*, *129*, 165–178. https://doi.org/10.1016/j.jafrearsci.2017.01.002

Tomonaga, Y., Brennwald, M. S., Meydan, A. F., & Kipfer, R. (2014). Noble gases in the sediments of Lake Van–solute transport and palaeoenvironmental reconstruction. *Quaternary Science Reviews*, *104*, 117–126. https://doi.org/10.1016/j.quascirev.2014.09.005

Topuz, G., Candan, O., Zack, T., & Yılmaz, A. (2017). East Anatolian plateau constructed over a continental basement: No evidence for the East Anatolian accretionary complex. *Geology*, *45*(9), 791–794. https://doi.org/10.1130/G39111.1

Uluocak, E. Ş. (2023). A discussion on geodynamic modeling methodology: Inferences from numerical models in the Anatolian Plate. *Geological Bulletin of Turkey*, 1–17. https://doi.org/10.25288/tjb.1318091

Uluocak, E. Ş. (2024). Dataset for "The role of upper mantle forces in post-subduction tectonics: Plumelet and active rifting in the East Anatolian Plateau" (G-Cubed). [Dataset]. *Zenodo*. https://doi.org/10.5281/zenodo.12568287

Uluocak, E. Ş., Göğüş, O. H., Pysklywec, R. N., & Chen, B. (2021). Geodynamics of East Anatolia-Caucasus domain: Inferences from 3D Thermo-mechanical models, residual topography, and admittance function analyses. *Tectonics*, *40*(12), e2021TC007031. https://doi.org/10.1029/2021TC007031

Uluocak, E. Ş., Pysklywec, R., & Göğüş, O. H. (2016). Present-day dynamic and residual topography in Central Anatolia. *Geophysical Journal International*, *206*(3), 1515–1525. https://doi.org/10.1093/gji/ggw225

Uluocak, E. Ş., Pysklywec, R. N., Göğüş, O. H., & Ulugergerli, E. U. (2019). Multidimensional geodynamic modeling in the Southeast Carpathians: Upper mantle flow-induced surface topography anomalies. *Geochemistry, Geophysics, Geosystems*, *20*(7), 3134–3149. https://doi.org/10.1029/2019GC008277

Uslular, G., & Gençalioğlu-Kuşcu, G. (2019). Geochemical characteristics of Anatolian basalts: Comment on "Neogene uplift and magmatism of Anatolia: Insights from drainage analysis and basaltic geochemistry" by McNab et al. *Geochemistry, Geophysics, Geosystems*, *20*(1), 530–541. https://doi.org/10.1029/2018gc007533

Uysal, I, Ersoy, E. Y., & Okay, A. I. (2021). Magmatic evolution and crustal growth of the Mediterranean region: New geochemical and geochronological perspectives. *Journal of Asian Earth Sciences*, *213*, 104769. https://doi.org/10.1016/j.jseaes.2021.104769

Van Hinsbergen, D. J., Torsvik, T. H., Schmid, S. M., Maţenco, L. C., Maffione, M., Vissers, R. L., et al. (2020). Orogenic architecture of the Mediterranean region and kinematic reconstruction of its tectonic evolution since the Triassic. *Gondwana Research*, *81*, 79–229. https://doi.org/10.1016/j.gr.2019.07.009

Wessel, P., Luis, J. F., Uieda, L., Scharroo, R., Wobbe, F., Smith, W. H. F., & Tian, D. (2019). The Generic Mapping Tools version 6. *Geochemistry, Geophysics, Geosystems*, *20*(11), 5556–5564. https://doi.org/10.1029/2019GC008515

White, R. S., & McKenzie, D. (1995). Mantle plumes and flood basalts. *Journal of Geophysical Research*, *100*(B9), 17543–17585. https://doi.org/10.1029/95jb01585

Whitehead, J. A., Jr., & Luther, D. S. (1975). Dynamics of laboratory diapir and plume models. *Journal of Geophysical Research*, *80*(5), 705–717. https://doi.org/10.1029/jb080i005p00705

Wilson, J. W., Roberts, G. G., Hoggard, M. J., & White, N. J. (2014). Cenozoic epeirogeny of the Arabian Peninsula from drainage modeling. *Geochemistry, Geophysics, Geosystems*, *15*(10), 3723–3761. https://doi.org/10.1002/2014GC005283

Yang, J., & Faccenda, M. (2020). Intraplate volcanism originating from upwelling hydrous mantle transition zone. *Nature*, *579*(7797), 88–91. https://doi.org/10.1038/s41586-020-2045-y

Yılmaz, Y., Şaroğlu, F., & Güner, Y. (1987). Initiation of the neomagmatism in East Anatolia. *Tectonophysics*, *134*(1–3), 177–199. https://doi.org/10.1016/0040-1951(87)90256-3

Zhu, H. (2018). High *Vp/Vs* ratio in the crust and uppermost mantle beneath volcanoes in the Central and Eastern Anatolia. *Geophysical Journal International*, *214*(3), 2151–2163. https://doi.org/10.1093/gji/ggy253

Zor, E. (2008). Tomographic evidence of slab detachment beneath eastern Turkey and the Caucasus. *Geophysical Journal International*, *175*(3), 1273–1282. https://doi.org/10.1111/j.1365-246x.2008.03946.x